Classes of geometrically generalized von Mises distributions

Thomas Dietrich*) and Wolf-Dieter Richter*)

*) Institute of Mathematics, University of Rostock, Ulmenstraße 69, 18057 Rostock, Germany

Abstract

Starting from a norm-contoured or star-shaped, bivariate vector distribution giving rise to a generalized radius coordinate, the conditional density of the polar angle given the fixed radius variable is derived and visualized. A model is fitted to real life data.

Keywords: conditional offset approach, model fit, directional coordinate, radius coordinate, norm contoured distribution, star-shaped distribution model, polygonally contoured model, non-concentric elliptically contoured model, p-generalized elliptically contoured model, density generating function, normalizing constant, unimodality, multimodality, symmetry, asymmetry, stochastic representations, process analysis, non-concentric elliptically contoured distributions

AMS Subject classification: 60E05

1 Introduction

The 2π-periodic function known as the von Mises density (vMd) arose from considering physical problems (Langevin [1905], von Mises [1918]). Applying a suitably adapted method of Gauss, nowadays called the maximum-likelihood method, von Mises [1918] was sucessfully searching for a cyclic error distribution. For a more detailed discussion, see, e.g., Gumbel et al. [1953].

Introductory and advanced results on and various applications of circular distributions and directional statistics can be found in Mardia [1972], Batschelet [1981], Fisher et al. [1987], Mardia and Jupp [2000], Jammalamadaka and SenGupta [2001], Pewsey et al. [2013], and the references given therein.

The conditional distribution of the directional component of a random vector given its fixed distance from the origin is often called a conditional offset distribution. Mardia [1972] showed by a construction following Fisher [1959] that the von Mises distribution (vMD) is the conditional distribution of the polar angle coordinate of a shifted, homoscedastic, regular, two-dimensional Gaussian random vector given its Euclidean radius coordinate. Jammalamadaka and SenGupta [2001] called this approach to the vMD the conditional offset approach. The conditional offset approach and its generalizations have been dealt with in Mardia and Jupp [2000], Shimizu and Iida [2002], Jones and Pewsey [2005], and Gatto and Jammalamadaka [2007].

The present paper contributes to the conditional offset approach under various aspects. First, we apply the it to a broad class of two-dimensional vector distributions, starting with shifted, possibly heteroscedastic Gaussian and elliptically contoured ones and then turning to norm contoured and star-shaped ones, we obtain a big class of Doing this, we obtain a big class of generalizations of the vMD. By introducing density generating functions we allow underlying bivariate distributions with heavy or light tails. By describing density levels with the help of positively homogeneous functions we deal with the aforementioned distributions.

Based on the study of rather general underlying bivariate models, we discuss the notions of a directional component (or coordinate) of a random vector and of the vector's generalized radius coordinate (or its generalized distance from the origin). We do this in accordance with the basic geometric properties of the two-dimensional density level sets of the underlying vector distribution. For a closely related comparison of the well interpretable polar and the more involved elliptical polar angle component of a Gaussian rv, we refer to Dietrich et al. [2013]. For different types of distances from the origin a random vector may have, see Richter [2011b, 2014, 2015] as well as Richter and Schicker [2016].

The radius component occuring in the conditional offset approach will be generally be non-Euclidean. However, the angular component will be the polar angle unless stated otherwise. For introductions to norm-contoured and star-shaped vector distributions, we refer to Richter [2015] and Richter [2014], respectively.

The paper is organized as follows. The conditional offset approach is presented for different choices of the parameters of the two-dimensional Gaussian distribution and for elliptically contoured vector distributions in Section 2. The resulting generalized vMds are visualized in Section 3. Also in Section 3, the four parameter model resulting in the Gaussian case is compared to two other four parameter models from the literature by means of maximum likelihood (ML) inference. The conditional offset approach for star-shaped bivariate model distributions is presented in Section 4 and the resulting generalized vMds are visualized in Section 5. According to Richter [2014], there is a need in the latter case to first determine the radius component of the bivariate random vectors in terms of Minkowski functionals of certain star bodies. This will be also done in Section 5. An example from the analysis of processing times deals with a polygonal generalization of the vMD. A concluding remark concerning statistical applications is added in Section 6.

2 conditional offset approach for Gaussian and elliptically contoured vector distributions

2.1 Axes-aligned Gaussian model

We write $(X,Y)^T \sim \Phi_{\nu,\Theta}$ if the rv $(X,Y)^T$ follows the Gaussian distribution having expectation vector $\nu \in \mathbb{R}^2$ and 2×2 covariance matrix Θ. Suppose that, for some $\lambda > 0$, $\delta > 0$, $\mu \in [-\pi, \pi)$ and $0 < b \leq a$,

$$(X,Y)^T \sim \Phi_{\lambda \begin{pmatrix} a\cos_{(a,b)}(\mu) \\ b\sin_{(a,b)}(\mu) \end{pmatrix}, \frac{1}{\delta}\begin{pmatrix} a^2 & 0 \\ 0 & b^2 \end{pmatrix}},$$

where $\cos_{(a,b)}(\varphi) = \cos\varphi/(a\,N_{(a,b)}(\varphi))$ and $\sin_{(a,b)}(\varphi) = \sin\varphi/(b\,N_{(a,b)}(\varphi))$ with

$$N_{(a,b)}(\varphi) = \left(\cos^2\varphi/a^2 + \sin^2\varphi/b^2\right)^{\frac{1}{2}}$$

are the $E_{(a,b)}$-generalized trigonometric functions introduced in Richter [2011a] and satisfying the equation $\cos^2_{(a,b)}(\varphi) + \sin^2_{(a,b)}(\varphi) = 1$, for all $\varphi \in \mathbb{R}$.

Changing from Cartesian to $E_{(a,b)}$-generalized elliptical polar coordinates $X = R\,a\cos_{(a,b)}(\Phi)$, $Y = R\,b\sin_{(a,b)}(\Phi)$, and denoting by $f_{(R,\Phi)}$ the probability density function (pdf) of the rv $(R,\Phi)^T$, it turns out that

$$f_{(R,\Phi)}(r,\varphi) = \frac{I_{[0,\infty)}(r) I_{[-\pi,\pi)}(\varphi)\,\delta r}{2\pi\,ab\,N^2_{(a,b)}(\varphi)} \times \exp\left\{-\frac{\delta}{2}\left[(r\cos_{(a,b)}(\varphi) - \lambda\cos_{(a,b)}(\mu))^2 + (r\sin_{(a,b)}(\varphi) - \lambda\sin_{(a,b)}(\mu))^2\right]\right\}$$

where I_A denotes the indicator function of the set A. Integrating $f_{(R,\Phi)}(r,\varphi)$ w.r.t. φ gives the marginal pdf f_R of R, and dividing $f_{(R,\Phi)}$ by f_R yields the conditional pdf of Φ given $R = r$,

$$f_{\Phi|R}(\varphi|r) = \frac{C_{(a,b,\delta r\lambda,\mu)}}{N^2_{(a,b)}(\varphi)} \exp\left\{\delta r\lambda\left[\cos_{(a,b)}(\varphi)\cos_{(a,b)}(\mu) + \sin_{(a,b)}(\varphi)\sin_{(a,b)}(\mu)\right]\right\}, \qquad (1)$$

where $C_{(a,b,\delta r\lambda,\mu)}$ is a normalizing constant such that $\int_{-\pi}^{\pi} f_{\Phi|R}(\varphi|r)\,d\varphi = 1$. Every choice of the triple (δ, r, λ) leading to the same product $\delta r\lambda = \kappa$, say, results in the same conditional pdf $f_{\Phi|R}$.

Moreover, since $\cos_{(a,b)}(\varphi) = \cos_{(1,b/a)}(\varphi)$, $\sin_{(a,b)}(\varphi) = \sin_{(1,b/a)}(\varphi)$ and $N_{(a,b)}(\varphi) = N_{(1,b/a)}(\varphi)/a$, we have $f_{\Phi|R}(\varphi|r) = \mathrm{vMd}_{\zeta,\kappa,\mu}(\varphi)$, where $\zeta = b/a$ and

$$\mathrm{vMd}_{\zeta,\kappa,\mu}(\varphi) = \frac{C_{(\zeta,\kappa,\mu)}}{N^2_{(1,\zeta)}(\varphi)} \exp\left\{\kappa\left[\cos_{(1,\zeta)}(\varphi)\cos_{(1,\zeta)}(\mu) + \sin_{(1,\zeta)}(\varphi)\sin_{(1,\zeta)}(\mu)\right]\right\} \tag{2}$$

with $C_{(\zeta,\kappa,\mu)}$ being the suitable normalizing constant. Note that Φ is the usual polar angle, but since $R = \left((X/a)^2 + (Y/b)^2\right)^{\frac{1}{2}}$, the conditioning in (1) is not a conditioning w.r.t. a multiple of the Euclidean radius unless $a = b$, i.e., $\zeta = 1$. See Richter [2011a] for more (geometric) explanation. If $\zeta = 1$, then $\cos_{(1,\zeta)} = \cos$, $\sin_{(1,\zeta)} = \sin$, $N_{(1,\zeta)}(\varphi) \equiv 1$, and, due to the well known formula

$$\cos\varphi\cos\mu + \sin\varphi\sin\mu = \cos(\varphi - \mu),$$

the pdf in (2) is that of the vMD with parameters κ and μ. This is the motivation for calling the 2π-periodic pdf in (2) the axes aligned elliptically contoured Gaussian generalized vMd with parameters $\zeta \in (0, 1], \kappa > 0$ and $\mu \in [-\pi, \pi)$. If $\zeta < 1$, then (2) may be also called the axes aligned heteroscedastic Gaussian generalization of the vMd.

Before we extend the conditional offset approach to the class of regular Gaussian vector distributions in Section 2.2, we state a Lemma which allows a more convenient representation of the normalizing constant.

Lemma 1. Let $T_{(a,b)} : \mathbb{R} \to \mathbb{R}$ be the mapping $\varphi \mapsto \psi$ defined by

$$T_{(a,b)}(\varphi) = \psi = \begin{cases} -\arccos(\cos_{(a,b)}(\varphi)) & -\pi \le \varphi < 0 \\ \arccos(\cos_{(a,b)}(\varphi)) & 0 \le \varphi < \pi \end{cases}$$

for some $a > 0$, $b > 0$, and $T_{(a,b)}(\varphi + 2\pi) = T_{(a,b)}(\varphi) + 2\pi$, $\forall\varphi$. Then $T_{(a,b)}$ is one-to-one, and $\cos_{(a,b)}(\varphi) = \cos(T_{(a,b)}(\varphi))$ and $\sin_{(a,b)}(\varphi) = \sin(T_{(a,b)}(\varphi))$, $\forall\varphi$. Moreover, the Jacobian of this transformation is $J_{T_{(a,b)}}(\varphi) = (ab\, N^2_{(a,b)}(\varphi))^{-1}$. The inverse map of the map $T_{(a,b)}$ is given by

$$T^{-1}_{(a,b)}(\psi) = \begin{cases} -\arccos(\cos_{(1/a,1/b)}(\psi)) & -\pi \le \psi < 0 \\ \arccos(\cos_{(1/a,1/b)}(\psi)) & 0 \le \psi < \pi \end{cases}, \quad T^{-1}_{(a,b)}(\psi + 2\pi) = T^{-1}_{(a,b)}(\psi) + 2\pi,\ \forall\psi\,.$$

Using Lemma 1, we conclude that $C_{(\zeta,\kappa,\mu)}$ does not depend on μ,

$$\begin{aligned} C_{(\zeta,\kappa,\mu)} &= \left(\int_{-\pi}^{\pi} N^{-2}_{(1,\zeta)}(\varphi)\, \exp\left\{\kappa\left[\cos_{(1,\zeta)}(\varphi)\cos_{(1,\zeta)}(\mu) + \sin_{(1,\zeta)}(\varphi)\sin_{(1,\zeta)}(\mu)\right]\right\}\, d\varphi\right)^{-1} \\ &= \left(\int_{-\pi}^{\pi} \zeta\, \exp\left\{\kappa\left[\cos\psi\cos(T_{(1,\zeta)}(\mu)) + \sin\psi\sin(T_{(1,\zeta)}(\mu))\right]\right\}\, d\psi\right)^{-1} \\ &= \left(\zeta\int_{-\pi}^{\pi} \exp\left\{\kappa\cos(\psi - T_{(1,\zeta)}(\mu))\right\}\, d\psi\right)^{-1} = \frac{1}{2\pi\,\zeta\, I_0(\kappa)}\,, \end{aligned}$$

i.e. $C_{(\zeta,\kappa,\mu)} = C_{(\zeta,\kappa)} = (2\pi\,\zeta\, I_0(\kappa))^{-1}$. The last integral in the evaluation of $C_{(\zeta,\kappa,\mu)}$ is the same as in the evaluation of the normalizing constant of the vMd having parameters κ and $T_{(1,\zeta)}(\mu)$. Here, $I_0(\kappa)$ is the modified Bessel function of the first kind and order zero, see, e.g., Abramowitz and Stegun [1972]. Hence, transforming $\Psi = T_{(1,\zeta)}(\Phi)$ yields the usual vMD. In light of Dietrich et al. [2013] and Richter [2014], one may prefer to consider the random polar angle Φ instead of the elliptic polar angle or eccentric anomaly Ψ, because of its easy interpretation.

2.2 Regular Gaussian model

The more general case that the Gaussian rv $(X, Y)^T$ has expectation vector ν and an arbitrary regular covariance matrix

$$\frac{1}{\delta}\,\Sigma = \frac{1}{\delta}\begin{pmatrix} \sigma_1^2 & \rho\sigma_1\sigma_2 \\ \rho\sigma_1\sigma_2 & \sigma_2^2 \end{pmatrix}$$

can be reduced to the preceding case as follows. The ellipse $E_\Sigma = \{(x,y)^T \in \mathbb{R}^2 : (x,y)\Sigma^{-1}(x,y)^T = 1\}$ can be rotated clockwise by the angle $\alpha \in [0, \pi/2)$ by multiplying it with the matrix $D(\alpha) = \left(\begin{smallmatrix} \cos\alpha & \sin\alpha \\ -\sin\alpha & \cos\alpha \end{smallmatrix}\right)$ such that the resulting ellipse $D(\alpha)E_\Sigma$ has main axes being aligned with the coordinate axes. To this end, the angle $\alpha = \alpha(\Sigma)$ has to be chosen according to formula (6) in Dietrich et al. [2013],

$$\begin{aligned}\alpha &= \alpha(\Sigma) \\ &= [1 - I_{\{0\}}(\rho)] \left[\frac{\pi}{4} I_{\{\sigma_2\}}(\sigma_1) + (1 - I_{\{\sigma_2\}}(\sigma_1)) \left(\frac{1}{2} \arctan \frac{2\sigma_1\sigma_2\rho}{\sigma_1^2 - \sigma_2^2} + \frac{\pi}{2} I_{(-\infty,0)}(\rho(\sigma_1 - \sigma_2)) \right) \right], \quad (3)\end{aligned}$$

where we define $2\sigma_1\sigma_2\rho/(\sigma_1^2 - \sigma_2^2) = sgn(\rho) \cdot \infty$ and $0 \cdot \arctan \pm\infty = 0$ if $\sigma_1 = \sigma_2$. The values a and b from the representation $D(\alpha)E_\Sigma = \{(x,y)^T \in \mathbb{R}^2 : (x/a)^2 + (y/b)^2 = 1\} = E_{(a,b)}$ are given also there in formula (7),

$$\begin{aligned} a = a(\Sigma) &= \sqrt{\sigma_1^2 \cos^2\alpha + \sigma_2^2 \sin^2\alpha + 2\rho\sigma_1\sigma_2 \sin\alpha\cos\alpha}\,, \\ b = b(\Sigma) &= \sqrt{\sigma_2^2 \cos^2\alpha + \sigma_1^2 \sin^2\alpha - 2\rho\sigma_1\sigma_2 \sin\alpha\cos\alpha}\,. \end{aligned} \quad (4)$$

Using the angle α according to (3) to change variables

$$X = \frac{R\cos\Phi}{N_{(a,b)}(\Phi - \alpha)}\,, \quad Y = \frac{R\sin\Phi}{N_{(a,b)}(\Phi - \alpha)}\,, \quad (5)$$

and following the conditional offset approach as before, leads to the conditional pdf of Φ given $R = r$,

$$\begin{aligned} f_{\Phi|R}(\varphi|r) &= \frac{C_{(a,b,\kappa,\mu)}(\alpha)}{N_{(a,b)}^2(\varphi - \alpha)} \\ &\quad \times \exp\left\{\kappa \left[\cos_{(a,b)}(\varphi - \alpha)\cos_{(a,b)}(\mu - \alpha) + \sin_{(a,b)}(\varphi - \alpha)\sin_{(a,b)}(\mu - \alpha)\right]\right\}, \quad (6) \end{aligned}$$

where $\alpha = \alpha(\Sigma)$, $a = a(\Sigma)$, $b = b(\Sigma)$ are given in (3) and (4), $\kappa = \delta r \lambda > 0$, the expectation vector of $(X,Y)^T$ is assumed to be

$$\nu = \frac{\lambda}{N_{(a,b)}(\mu - \alpha)} \begin{pmatrix} \cos\mu \\ \sin\mu \end{pmatrix}$$

for some $\mu \in [-\pi, \pi)$ and $\lambda > 0$, and where the normalizing constant does not depend on α and μ, $C_{(a,b,\kappa,\mu)}(\alpha) = C_{(a,b,\kappa)}$. Again, every choice of the triple (δ, r, λ) leading to the same product κ results in the same conditional pdf $f_{\Phi|R}$. Note that Φ is still the usual random polar angle of $(X,Y)^T$. However, the conditioning random radius coordinate is now the elliptical radius $R = h_{K_\Sigma}((X,Y)^T)$, where

$$h_K((x,y)^T) = \inf\{\xi > 0 : (x,y)^T \in \xi \cdot K\}$$

defines the Minkowski functional of a star body K having the origin as an inner point, and

$$K_\Sigma = \left\{(x,y)^T \in \mathbb{R}^2 : (x,y)\Sigma^{-1}(x,y)^T \le 1\right\}$$

is the star body circumscribed by the ellipse E_Σ. Note that R is the Euclidean radius if Σ is the 2×2 unit matrix. In the general case, however, $R = R(\Phi) = (X^2 + Y^2)^{\frac{1}{2}} N_{(a,b)}(\Phi - \alpha)$, where $\tan\Phi = Y/X$, and α is defined in (3).

Note that, contrary to Sections 2.1 and 2.2, the quantities a und b defined in (4) do not satisfy any certain inequality yet. However, using the equalities $\cos_{(a,b)}(\varphi) = -\sin_{(b,a)}(\varphi - \pi/2)$, $\sin_{(a,b)}(\varphi) =$

$\cos_{(b,a)}(\varphi - \pi/2)$ and $N^2_{(a,b)}(\varphi) = N^2_{(b,a)}(\varphi - \pi/2)$, $\forall\varphi$, the right side of the equation in (6) can be rewritten as

$$\frac{C_{(a,b,\kappa)}\, \exp\left\{\kappa\left[\cos_{(b,a)}(\varphi-\alpha^*)\cos_{(b,a)}(\mu-\alpha^*) + \sin_{(b,a)}(\varphi-\alpha^*)\sin_{(b,a)}(\mu-\alpha^*)\right]\right\}}{N^2_{(b,a)}(\varphi-\alpha^*)},$$

where $\alpha^* = \alpha + \pi/2 \in [\pi/2, \pi)$. The latter representation of (6) corresponds to the case where the ellipse E_Σ is rotated clockwise by the angle $\alpha^* = \alpha + \pi/2$ instead of α, $D(\alpha^*)E_\Sigma = E_{(b,a)}$, cf. Remark 6.2 in Dietrich et al. [2013].

In accordance with Section 2.1 we may use α^* instead of α whenever $a < b$ to ensure that the main axis aligned with the x-axis is not the smaller one. Enlarging the domain of α up to the interval $[0, \pi)$ this way, we have $f_{\Phi|R}(\varphi|r) = \mathrm{vMd}_{\zeta,\kappa,\mu,\alpha}(\varphi)$, where again $\zeta = b/a$,

$$\begin{aligned}\mathrm{vMd}_{\zeta,\kappa,\mu,\alpha}(\varphi) &= \frac{C_{(\zeta,\kappa)}}{N^2_{(1,\zeta)}(\varphi-\alpha)} \\ &\quad\times \exp\left\{\kappa\left[\cos_{(1,\zeta)}(\varphi-\alpha)\cos_{(1,\zeta)}(\mu-\alpha) + \sin_{(1,\zeta)}(\varphi-\alpha)\sin_{(1,\zeta)}(\mu-\alpha)\right]\right\}, \qquad (7)\end{aligned}$$

and $C_{(\zeta,\kappa)} = (2\pi\,\zeta\, I_0(\kappa))^{-1}$. The 2π-periodic pdf in (7) will be called the regular Gaussian elliptically contoured generalization of the vMd having paramaters $\zeta \in (0, 1]$, $\kappa > 0$, $\mu \in [-\pi, \pi)$ and $\alpha \in [0, \pi)$.

2.3 A class of representations for the vMD

Before we turn over to the elliptically contoured model in Section 2.4, we want to draw some consequences from our considerations so far. Given any regular bivariate Gaussian random vector and any fixed value $r > 0$ of the conditioning random elliptical radius R, the conditional offset approach uniquely defines a regular Gaussian elliptically contoured generalization of the vMD. Moreover, with regard to Lemma 1, such a generalized vMD is associated with an uniquely determined vMD having parameters $\kappa > 0$ and $\nu \in [-\pi, \pi)$. Consequently, any regular bivariate Gaussian distribution is thus uniquely related to a vMD. The next theorem emphasizes this fact by stating a class of representations for any vMD with parameters $\kappa > 0$ and $\nu \in [-\pi, \pi)$.

Let $T_{(a,b)}$ denote the map considered in Lemma 1 for some fixed $0 < b \leq a$, and define $|(x, y)^T|_{(a,b)} := (x^2/a^2 + y^2/b^2)^{1/2}$, following the notation in Richter [2011a].

Theorem 2.1. Let a random variable Ψ follow a vMD with arbitrary but fixed parameters $\kappa > 0$ and $\nu \in [-\pi, \pi)$, and let the polar angle of $(x, y)^T \neq (0, 0)^T$ be $\mathrm{Pol}^{*-1}(x, y)$. Then

$$\mathcal{L}(\Psi) = \mathcal{L}\big(T_{(a,b)}(\mathrm{Pol}^{*-1}(X, Y)) \mid |D(\alpha)(X, Y)^T|_{(a,b)} = r\big)$$

for all Gaussian random vectors $(X, Y)^T$,

$$(X, Y)^T \sim \Phi_{\frac{\lambda}{N_{(a,b)}(\mu-\alpha)}\begin{pmatrix}\cos\mu\\ \sin\mu\end{pmatrix}, D^T(\alpha)\begin{pmatrix}a^2 & 0\\ 0 & b^2\end{pmatrix}D(\alpha)},$$

where $r > 0$ and $\lambda > 0$ satisfy $\kappa = r\lambda$, and $\mu \in [-\pi, \pi)$ and $\alpha \in [0, \pi)$ are such that $T_{(a,b)}(\mu - \alpha) \equiv \nu$ modulo 2π.

Remark 1. Let Ψ follow a vMD with arbitrary parameter $\kappa > 0$ and $\nu = 0$, and fix $0 < b \leq a$. Then, for any $\mu \in [-\pi, \pi)$ and $\alpha \in [0, \pi)$, it follows that $\mathcal{L}(T^{-1}_{(a,b)}(\Psi + T_{(a,b)}(\mu - \alpha)) + \alpha)$ coincides with the regular Gaussian elliptically contoured generalization of the vMD having parameters $\zeta = b/a$, $\kappa > 0$, μ and α by simple density transformation.

Kato and Jones [2010] consider a Möbius transformation M which maps the unit circle onto itself in the complex plane. With respect to the arguments of the corresponding complex numbers ψ and φ, say, such a circle-to-circle transformation is given there by

$$\psi \overset{M}{\longmapsto} \varphi = \mu + \nu + 2\arctan\left(\frac{1-r}{1+r}\tan\left(\frac{\psi-\nu}{2}\right)\right), \quad \psi \in [0, 2\pi) \qquad (8)$$

where $\mu, \nu \in [0, 2\pi)$ and $r \in [0, 1)$. We further require $\psi + 2\pi \mapsto \varphi + 2\pi$, for any ψ. Using the Möbius transformation from Ψ to $\Phi = M(\Psi)$, Kato and Jones [2010] discuss the resulting family of four-parameter distributions on the circle. We remark that there is no Möbius transformation M given in (8) which leads to a regular Gaussian elliptically contoured generalization of the vMD unless for the special subcase $a = b$, i.e. $\zeta = 1$. This is a consequence of the following symmetry properties of the continuous and strictly monotonically increasing transformations under consideration. The transformation $T^*_{(a,b)}$ defined by

$$\psi \overset{T^*_{(a,b)}}{\longmapsto} \varphi = T^{-1}_{(a,b)}(\psi + T_{(a,b)}(\mu - \alpha)) + \alpha \tag{9}$$

is symmetric w.r.t. any of the points $(-T_{(a,b)}(\mu - \alpha) + k\pi/2, \alpha + k\pi/2)$, $k \in \mathbb{Z}$. Here, $\mathbb{Z}$ denotes the set of all integers. Hence, all points of symmetry are equidistantly spread on a straight line having slope one. If $r > 0$, the transformation (8) is only symmetric with respect to any of the points $(\nu + k2\pi, \mu + \nu + k2\pi)$, $k \in \mathbb{Z}$, which again are equidistantly spread on a straight line having slope one, see Figure 1. Consequently, if $r \in (0, 1)$, we can only find three such points of symmetry if ψ runs through any closed interval of length 2π. Considering (9), we can find five such points. Therefore, transforming Ψ according to (8) or (9), respectively, results in different circular distributions. The special case of $r = 0$ entails the simple linear transformation $\psi \mapsto \mu + \nu + (\psi - \nu)/2$. Hence, if $r = 0$ and $a = b$, then (8) as well as (9) transform Ψ to a von Mises distributed random variable.

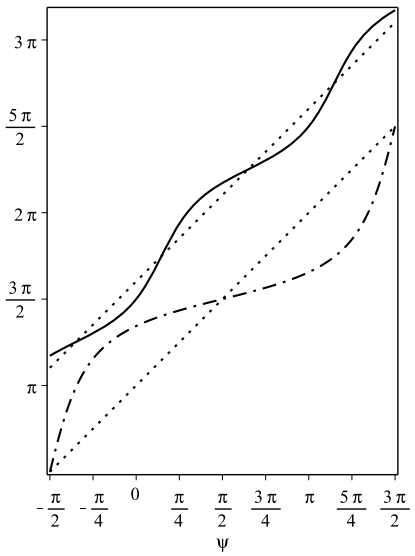

Figure 1: The graph of $T^*_{(a,b)}$ (solid) with $a = 2$, $b = 1$, $\mu_1 = 3\pi/2$, $\alpha = \pi/4$ and the graph of the Möbius transformation M (dash-dotted) with $r = 0.6$, $\mu_2 = \pi$, $\nu = \pi/2$ in the interval $[\nu - \pi, \nu + \pi]$. Both functions are symmetric with respect to any intersection points with the corresponding dotted line. Note that both transformations map $[\nu - \pi, \nu + \pi)$ onto an interval of length 2π.

2.4 Elliptically contoured model

Let $g : [0, \infty) \to [0, \infty)$ satisfy $0 < I(g) < \infty$ where $I(g) = \int_0^\infty r g(r)\, dr$. Any such function will be called a density generating function (dgf). We write $(X, Y)^T \sim \Phi_{g,\nu,\Theta}$ if $(X, Y)^T$ has the pdf

$$(x, y)^T \mapsto D(g) \cdot |\Theta|^{-\frac{1}{2}} \cdot g\left(\left((x - \nu_1, y - \nu_2)\Theta^{-1}(x - \nu_1, y - \nu_2)^T\right)^{\frac{1}{2}}\right) \tag{10}$$

where $\nu = (\nu_1, \nu_2)^T \in \mathbb{R}^2$, Θ is a 2×2 symmetric positive definite matrix and $D(g)$ is a suitable normalizing constant. In other words, $(X, Y)^T$ follows an elliptically contoured distribution with expectation vector ν, shape matrix Θ and dgf g.

Note that the conditional offset approach to the Gaussian elliptically contoured generalized vMd can be adapted to any absolutely continuous elliptically contoured distribution. For the subclass of spherically symmetric distributions, where Θ is a multiple of the unit matrix, this idea is outlined in Jones and Pewsey [2005]. To this end, let $(X,Y)^T \sim \Phi_{g,\nu,\frac{1}{\delta}\Sigma}$. Changing variables according to (5) where again $\alpha = \alpha(\Sigma)$, $a = a(\Sigma)$ and $b = b(\Sigma)$ are given as in (3) and (4), respectively, and following the conditional offset approach, we arrive at the conditional pdf of the polar angle Φ given the fixed value of the elliptical radius $R = r$,

$$f_{\Phi|R}(\varphi|r) = \frac{C_{(a,b,\delta,r,\lambda,\mu)}(\alpha, g)}{N^2_{(a,b)}(\varphi - \alpha)} \times g\left(\left(\delta(r^2+\lambda^2) - 2\delta r\lambda\left[\cos_{(a,b)}(\varphi-\alpha)\cos_{(a,b)}(\mu-\alpha) + \sin_{(a,b)}(\varphi-\alpha)\sin_{(a,b)}(\mu-\alpha)\right]\right)^{\frac{1}{2}}\right). \tag{11}$$

The parameters λ and μ are uniquely defined by the representation of the expectation vector ν of $(X,Y)^T$,

$$\nu = \frac{\lambda}{N_{(a,b)}(\mu-\alpha)}\begin{pmatrix}\cos\mu\\ \sin\mu\end{pmatrix}.$$

The normalizing constant $C_{(a,b,\delta,r,\lambda,\mu)}(\alpha, g)$ does actually neither depend on α nor on μ. Notice that, in contrast to the Gaussian case, the density in (11) generally depends not only through the product $\delta r\lambda$ on the triple (δ, r, λ). However, replacing the triple (δ, r, λ) by $(1, \sqrt{\delta}r, \sqrt{\delta}\lambda)$ and exchanging the roles of r and λ yields the same density. These are the reasons why we assume w.l.o.g. that $\delta = 1$ and $\lambda \geq r$, from now on. The conditional pdf $f_{\Phi|R}$ depends only through $\zeta = b/a$ upon a and b, thus we arrived at $f_{\Phi|R}(\varphi|r) = \mathrm{vMd}_{g;\zeta,r,\lambda,\mu,\alpha}(\varphi)$, where the 2π-periodic pdf

$$\mathrm{vMd}_{g;\zeta,r,\lambda,\mu,\alpha}(\varphi) = \frac{C_{(\zeta,r,\lambda)}(g)}{N^2_{(1,\zeta)}(\varphi-\alpha)} \times g\left(\left(r^2+\lambda^2 - 2r\lambda\left[\cos_{(1,\zeta)}(\varphi-\alpha)\cos_{(1,\zeta)}(\mu-\alpha) + \sin_{(1,\zeta)}(\varphi-\alpha)\sin_{(1,\zeta)}(\mu-\alpha)\right]\right)^{\frac{1}{2}}\right) \tag{12}$$

is called the regular elliptically contoured g-generalization of the vMd having parameters $\zeta \in (0,1]$, $0 < r \leq \lambda$, $\mu \in [-\pi, \pi)$ and $\alpha \in [0, \pi)$. The fact that $\zeta \in (0,1]$ is again a consequence of the circumstance that the original domain of α was enlarged, cf. Section 2.2. By means of Lemma 1, the normalizing constant $C_{(\zeta,r,\lambda)}(g)$ can be simplified as

$$C_{(\zeta,r,\lambda)}(g) = \left(\zeta\int_{-\pi}^{\pi} g\left(\left(r^2+\lambda^2-2r\lambda\cos\psi\right)^{\frac{1}{2}}\right)\,d\psi\right)^{-1}. \tag{13}$$

Note that the latter integral equals that arising in the evaluation of the normalizing constant in the spherical case in Jones and Pewsey [2005], Section 2.5. The elliptical polar angle $\Psi = T_{(1,\zeta)}(\Phi)$, with suitably chosen parameters, has the distribution considered also there. Since we study the conditional pdf of the polar angle Φ given the elliptical radius, instead of studying the elliptical polar angle Ψ given the Euclidean radius, the resulting distribution classes allow rather different interpretation and are actually not limited to symmetric pdfs, here. However, any regular elliptically contoured g-generalized vMd (in the sense of the present work) which involves symmetry can be identified as a g-generalization in the sense of Jones and Pewsey [2005].

Note that the density $\mathrm{vMd}_{g;\zeta,r,\lambda,\mu,\alpha}$ defined in (12) where $\alpha \neq 0$ can be represented as a shifted version of the density $\mathrm{vMd}_{g;\zeta,r,\lambda,\mu-\alpha,0}$,

$$\mathrm{vMd}_{g;\zeta,r,\lambda,\mu,\alpha}(\varphi) = \mathrm{vMd}_{g;\zeta,r,\lambda,\mu-\alpha,0}(\varphi-\alpha), \quad \text{for all } \varphi.$$

Here, $\mu - \alpha$ may be altered modulo 2π with respect to the domain $[-\pi, \pi)$ of the parameter. Moreover, the argument of the dgf g in (12) is a 2π-periodic continuous function

$$\varphi \mapsto \left(r^2+\lambda^2-2r\lambda\left[\cos_{(1,\zeta)}(\varphi-\alpha)\cos_{(1,\zeta)}(\mu-\alpha) + \sin_{(1,\zeta)}(\varphi-\alpha)\sin_{(1,\zeta)}(\mu-\alpha)\right]\right)^{\frac{1}{2}}$$

taking all values from the interval $[\lambda - r, \lambda + r]$. The global maximum and minimum points of this function do not depend on $\zeta \in (0, 1]$, and are given by $\mu + k2\pi$ and $\mu + \pi + k2\pi$, respectively, where $k \in \mathbb{Z}$. Hence, $f_{\Phi|R}(\varphi|r)$ depends on g only through its values in this interval. If the dgf is $g = g_G$, $g_G(r) = \exp\left\{-r^2/2\right\}$, $r > 0$, then $(X, Y)^T$ follows a Gaussian distribution, and the conditional pdf of Φ given $R = r$ is the regular Gaussian elliptically contoured generalization of the vMd.

By suitable choices of the dgf g, one can model bivariate elliptically contoured distributions with heavy or light tails. Moreover, different degree of concentration of probability mass of $(X, Y)^T$ at the expectation vector $\nu \in \mathbb{R}^2$ may be modeled this way. Frequently used dgfs are that of Kotz type or Pearson type VII,

$$g_K(r) = r^{2(M-1)} \exp\left\{-\beta r^{2\gamma}\right\}, \quad M > 0, \beta > 0, \gamma > 0,$$
$$g_P(r) = \left(1 + \frac{r^2}{m}\right)^{-M}, \quad M > 1, m > 0,$$

respectively, where $r > 0$. The dgf g_G of the Gaussian distribution belongs to the Kotz type class of dgfs and entails light tails. On the other hand, the dgf $g_t(r) = (1 + r^2/m)^{-m/2-1}$, $m > 0$ of the multivariate t-distribution is a special Pearson type VII dgf which models heavier tails.

For evaluating the regular elliptically contoured g-generalization of the vMd one seeks for an explicit representation of the normalizing constant $C_{(\zeta,r,\lambda)}(g)$ as in (13). Changing variables $\psi = 2\alpha$, one can exploit the well known relation $\cos(2\alpha) = 2\cos^2\alpha - 1$ to get

$$\frac{1}{C_{(\zeta,r,\lambda)}(g)} = 2\zeta \int_{-\pi/2}^{\pi/2} g\left(((r+\lambda)^2 - 4r\lambda\cos^2\alpha)^{1/2}\right) d\alpha.$$

In the case of a Kotz type dgf one can consider the power series expansion of the exponential term, and interchange the order of integration and summation,

$$\begin{aligned}\frac{1}{C_{(\zeta,r,\lambda)}(g_K)} &= 2\zeta \cdot \sum_{m=0}^{\infty} \frac{(-\beta)^m}{m!} \int_{-\pi/2}^{\pi/2} \left((r+\lambda)^2 - 4r\lambda\cos^2\alpha\right)^{\gamma m + M - 1} d\alpha \\ &= 2\zeta\,\pi \cdot \sum_{m=0}^{\infty} \frac{(-\beta)^m}{m!} \frac{{}_2F_1\left(\frac{1}{2}, 1 - \gamma m - M; 1; \frac{4r\lambda}{(\lambda+r)^2}\right)}{(r+\lambda)^{2(1-\gamma m - M)}}, r \neq \lambda,\end{aligned}$$

where the last equation follows from 3.682 in Gradshteyn and Ryzhik [2007], and ${}_2F_1$ is the Gaussian hypergeometric function which is available as a standardly implemented function in software packages like MATLAB and Maple. If $r = \lambda$ then

$$\begin{aligned}\frac{1}{C_{(\zeta,r,\lambda)}(g_K)} &= 2\zeta \cdot \sum_{m=0}^{\infty} \frac{(-\beta)^m}{m!} \int_{-\pi/2}^{\pi/2} \left(4r^2 - 4r^2\cos^2\alpha\right)^{\gamma m + M - 1} d\alpha \\ &= 2\zeta\sqrt{\pi} \cdot \sum_{m=0}^{\infty} \frac{(-\beta)^m}{m!} \frac{(4r^2)^{\gamma m + M - 1}\Gamma\left(m\gamma + M - \frac{1}{2}\right)}{\Gamma(m\gamma + M)},\end{aligned}$$

where we exploited an integral representation of the beta function (Gradshteyn and Ryzhik [2007], 8.380 (2)) which can subsequently be written in terms of gamma functions.

In the case of a Pearson type VII dgf, it follows again from 3.682 in Gradshteyn and Ryzhik [2007] that

$$\begin{aligned}\frac{1}{C_{(\zeta,r,\lambda)}(g_P)} &= 2\zeta \int_{-\pi/2}^{\pi/2} \left(1 + \frac{(r+\lambda)^2 - 4r\lambda\cos^2(\alpha)}{m}\right)^{-M} d\alpha \\ &= \frac{2\zeta\,\pi\,{}_2F_1\left(\frac{1}{2}, M; 1; \frac{4\lambda r}{m + (r+\lambda)^2}\right)}{\left(\frac{m + (r+\lambda)^2}{m}\right)^M}.\end{aligned}$$

3 Visualization of the elliptically contoured generalized vMd

This section provides some visualizations of the generalized vMd for the elliptically contoured model. First, the axes aligned and the general regular Gaussian cases will be illustrated, for which the densities are given in (2) and (7), respectively. The effectiveness of the four parameter model (7) is shown by applying it to real life data. Then, elliptically contoured g-generalizations of the vMd are drawn for $g \in \{g_K, g_P\}$. Recall that circular densities are 2π-periodic by definition. That is why we illustrate circular densities only in intervals of length 2π. However, one has always to keep in mind the 2π-periodic nature of the pdf to not get the impression of asymmetry even in cases when the density is symmetric, see Figure 10.

3.1 Gaussian elliptically contoured generalizations of the vMd

Except for Figure 6, the figures in the present section deal with the axes aligned Gaussian case. In this case, the dgf is g_G and the shift parameter is $\alpha = 0$. The three parameters ζ, κ and μ are of influence for the shape of the generalized vMd. Altering in each figure only one of these parameters, Figures 2 and 3 show that the density can be unimodal symmetric (cf. Jones and Pewsey [2005]) and unimodal asymmetric. Alternatively, Figures 4 and 5 show examples of both symmetric and asymmetric bimodality. Recall that $\zeta = 1$ always entails symmetry, see Figure 5.

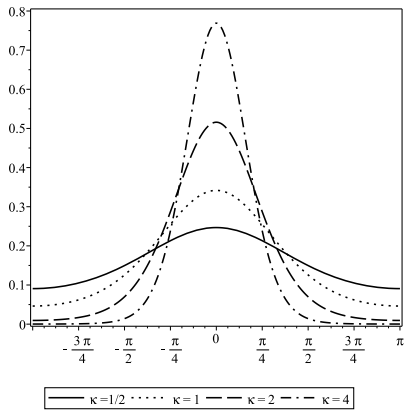

Figure 2: $\zeta = 1, \mu = 0$

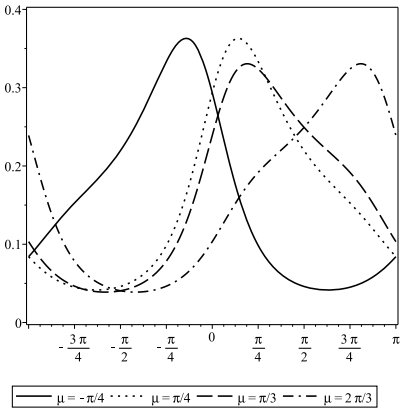

Figure 3: $\zeta = 4/5, \kappa = 1$

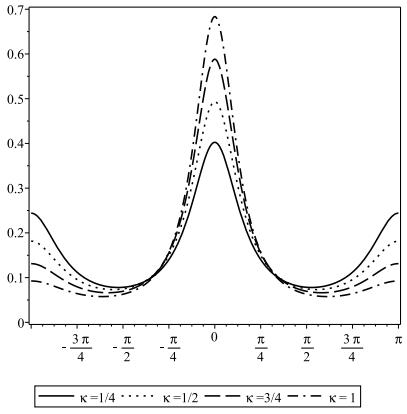

Figure 4: $\zeta = 1/2, \mu = 0$

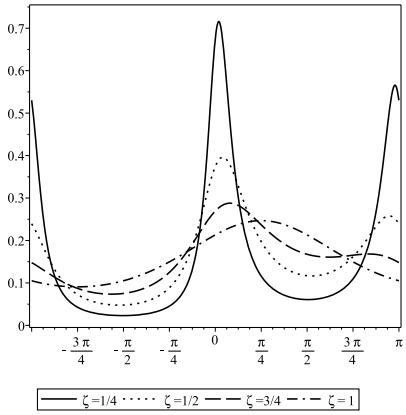

Figure 5: $\kappa = 1/2, \mu = \pi/4$

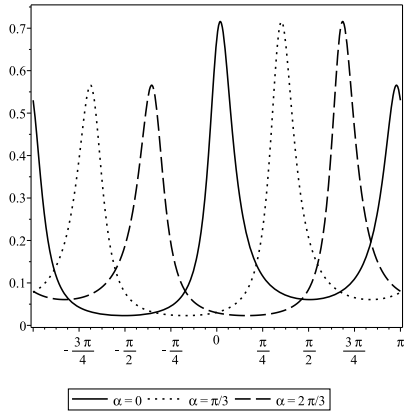

Figure 6: $\zeta = 1/4, \kappa = 1/2, \mu = \pi/4 + \alpha$

All figures discussed so far deal with the case $\alpha = 0$, i.e. with the axes aligned case. The case $\alpha \neq 0$ can be considered as a shifted version of the densities drawn already in Section 2.4 and Figure 6. Therefore, the visualization of such shifts is omitted in the rest of the paper.

3.2 Fitting and comparing the regular Gaussian model

We consider now fitting the regular Gaussian elliptically contoured generalization of the vMd to real life data by means of ML inference. Let the log-likelihood function based on an iid sample from density (7) be denoted by l. We do not introduce here the system of equations the ML estimators $\hat{\zeta}, \hat{\kappa}, \hat{\mu}$ and $\hat{\alpha}$ must satisfy. Instead, we directly minimize the negative log-likelihood. This can efficiently be done with the help of the MATLAB routine *fminsearch*. Since one cannot guarantee uniqueness of a local minimum of $-l$, we let run *fminsearch* several times where the starting values of all the parameters are chosen randomly, each time. In addition to model (7), we consider two competing four parameter models being also generalizations of the vMD. The generalized von Mises distribution GvM_2 considered in Gatto and Jammalamadaka [2007] has a pdf proportional to

$$\exp\{\kappa_1 \cos(\varphi - \mu_1) + \kappa_2 \cos(2(\varphi - \mu_2))\}, \quad \varphi \in [0, 2\pi), \tag{14}$$

where $\mu_1 \in [0, 2\pi)$, $0 \leq \mu_2 < \pi$ and $\kappa_1, \kappa_2 > 0$. For the pdf

$$\frac{1 - r^2}{2\pi\, I_0(\kappa_3)} \exp\left\{ \frac{\kappa_3 \left(\xi \cos(\varphi - \eta) - 2r \cos\nu\right)}{1 + r^2 - 2r \cos(\varphi - \gamma)} \right\} \frac{1}{1 + r^2 - 2r \cos(\varphi - \gamma)}, \quad \varphi \in [0, 2\pi) \tag{15}$$

where γ, ξ and η are functions of the four parameters $\mu_3, \nu \in [0, 2\pi), r \in [0, 1)$ and $\kappa > 0$, see Kato and Jones [2010]. Note that we have considered already in Section 2.3 the Möbius transformation associated with (15) . For comparing several models, Kato and Jones [2010] considered the Akaike (AIC) and Bayes information criterions (BIC) which are based on the log-likelihood l and on a penalty term depending on the number of estimated parameters and, in case of BIC, also on the number of observations. For more details on AIC and BIC, we refer to Burnham and Anderson [2002]. Since all the models under consideration here have the same number of parameters, there is no need for calculating the AIC or BIC. Thus we can compare all three models directly according to their maximized log-likelihood. The calculation of the ML estimators is always based on several restarts of the routine *fminsearch* which we adopted from Gatto and Jammalamadaka [2007]. Our comparative study is based on data sets that have already been considered in Gatto and Jammalamadaka [2007] or Kato and Jones [2010], respectively. First, we consider data taken from a regional, integrated hydrological monitoring system for the pan-Arctic land mass called ArcticRIMS, accessible at the WWW address `http://rims.unh.edu/`. This project provides a near-real time monitoring of pan-Arctic water budgets and river discharge to the Arctic Ocean which are important elements of the larger Earth System especially with regard to global climate change. Among several other variables the wind directions are measured at several locations. Gatto and Jammalamadaka [2007] considered the wind directions measured daily from January 2005 to December 2005 on four different sites at continental level: the Pan Arctic, the Europe, the Greenland and the North America basins. These data sets and the related MATLAB programs from Gatto are available at `http://www.imsv.unibe.ch/content/research/publications/software/index_eng.html`.

The data set considered in Kato and Jones [2010] concerns wind directions measured hourly between July 1 and 31, 2007, at Neuglobsow (Germany) by an integrated monitoring station for atmospheric observations that belongs to the Umweltbundesamt (German Federal Environment Agency). The full data set is available from the WMO World Data Centre for Greenhouse Gases at the WWW address `http://ds.data.jma.go.jp/gmd/wdcgg/` (search the data catalogue for Neuglobsow, MET (Meteorological Data)).

Table 1 shows the ML estimates of the parameters and the maximized log-likelihood. According to the latter, model (7) is the most competitive one for all four data sets taken from ArcticRIMS. Notice that the log-likelihood regarding model (14) for the Greenland Basins is improved compared to the ML estimates given in Gatto and Jammalamadaka [2007]. With respect to the data from Neuglobsow, density (15) fits best. However, model (7) fits nearly as good as (15) and better than (14) by some distance although it also inserts in its graph an unsupportable 'shoulder' around 2.5 radians, cf. Kato and Jones [2010]. According to Kato and Jones [2010], model (14) is to be preferred in favour of (15) when bimodality is expected, see the log-likelihood in Table 1. If there

Table 1: ML estimates of the parameters and the maximized log-likelihood

model (7)	$\hat{\zeta}$	$\hat{\kappa}$	$\hat{\mu}$	$\hat{\alpha}$	l
Pan Arctic basins	0.2174	1.0428	−2.1130	0.9893	**−337.1615**
Europe basins	0.2705	0.3829	−2.2217	0.8499	**−492.4967**
Greenland basins	0.2929	0.2484	−0.4414	0.9353	**−544.1206**
North America basins	0.2065	0.3332	−2.0187	1.0199	**−440.3798**
Neuglobsow	0.5553	1.3182	−1.7645	1.8110	−1009.2287
GJ model (14)	$\hat{\kappa}_1$	$\hat{\kappa}_2$	$\hat{\mu}_1$	$\hat{\mu}_2$	l
Pan Arctic basins	0.8109	1.9897	4.5055	0.9822	−378.5888
Europe basins	0.2781	1.6028	4.2329	0.8530	−499.8043
Greenland basins	0.4085	1.2521	5.7489	0.9550	−558.6433
North America basins	0.3444	1.8600	4.9710	1.0082	−468.2882
Neuglobsow	1.3002	0.6327	4.1054	1.7966	−1024.0578
KJ model (15)	$\hat{\kappa}_3$	$\hat{r}$	$\hat{\nu}$	$\hat{\mu}_3$	l
Pan Arctic basins	1.7939	0.7827	2.2916	2.2224	−401.2495
Europe basins	2.9116	0.6579	3.4999	5.8278	−575.9140
Greenland basins	2.4629	0.5312	3.1483	5.7410	−617.1228
North America basins	3.1643	0.6893	2.8138	2.2969	−572.7837
Neuglobsow	1.8201	0.5052	2.2105	3.3130	**−1006.7217**

is no particular reason to expect bimodality, but there is evidence of asymmetry, model (15) seems to be more attractive to Kato and Jones [2010] than (14). The numerical illustration yields the confidence for the new model (7) being competitive in both situations and being even better than (14) for the data considered here, when bimodality is expected. Note that the normalizing constant in (7) is easy to handle whereas the normalizing constant in (14) is an infinite sum of products of modified Bessel functions. Figure 7 shows the fitted densities and the superposed histograms of the corresponding wind directions. For the purposes of comparability with the literature, the densities are considered on the interval $[0, 2\pi)$. We adopted the number of bins as good as possible from Gatto and Jammalamadaka [2007] (≈ 62 bins) and Kato and Jones [2010] (12 bins).

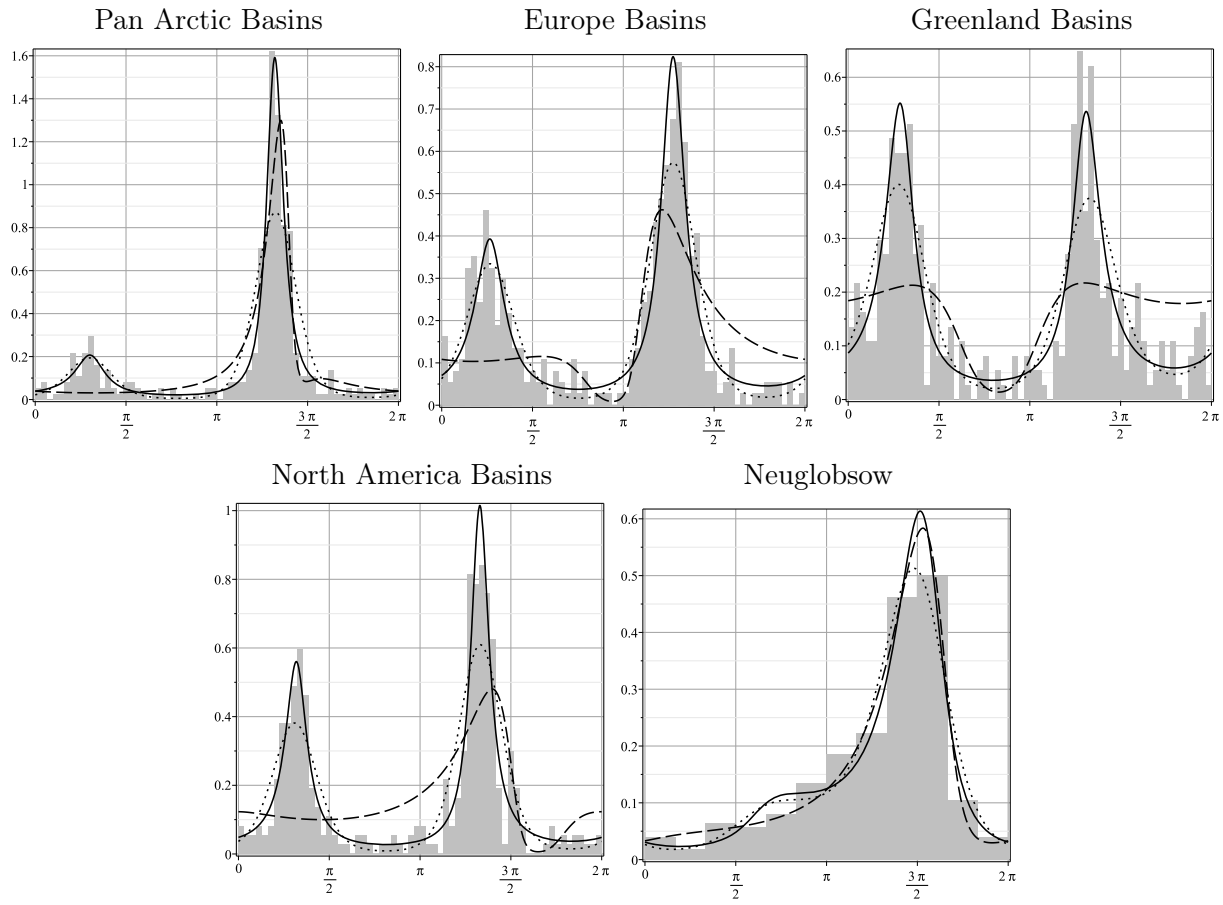

Figure 7: Fitted densities as in (7) [solid], (14) [dotted] and (15) [dashed]

3.3 Elliptically contoured generalizations of the vMd

In real data applications, it may be of some interest to adapt just a small number of parameters instead of a completely unknown type of dgf. This section deals with two parameterized families of dgfs and the generalized vMDs based upon the corresponding bivariate probability laws.

3.3.1 The Kotz type generalization $\mathrm{vMd}_{g_K;\zeta,r,\lambda,\mu,\alpha}$

Let $g = g_K$ in (12), where g_K involves the additional parameters $M > 1/2$, $\beta > 0$ and $\gamma > 0$. Note that $\mathrm{vMd}_{g;\zeta,r,\lambda,\mu,\alpha}$ does not change if we replace (r, λ, β) by $((2\beta)^{1/(2\gamma)}r, (2\beta)^{1/(2\gamma)}\lambda, 1/2)$, and that $\beta = 1/2, M = \gamma = 1$ corresponds to the Gaussian case. That is why we put w.l.o.g. $\beta = 1/2$ and are further only concerned with the remaining parameters $\zeta, r, \lambda, \mu, M$ and γ. Of course, one can reproduce all the figures from the preceding Gaussian case here as well. But in addition, Figure 8 shows bimodal density functions which are pretty much concentrated on the interval $[0, \pi)$ if $\gamma \geq 2$. One can also model three modes, see Figure 9.

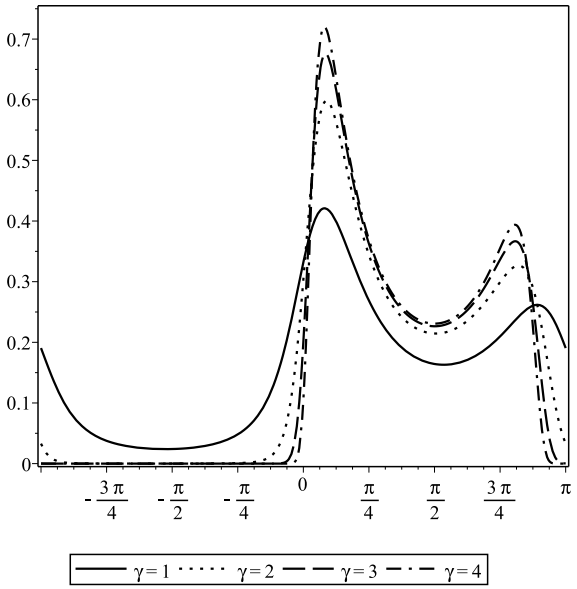

Figure 8: $\zeta = 1/2, r = \lambda = M = 1, \mu = \pi/3$

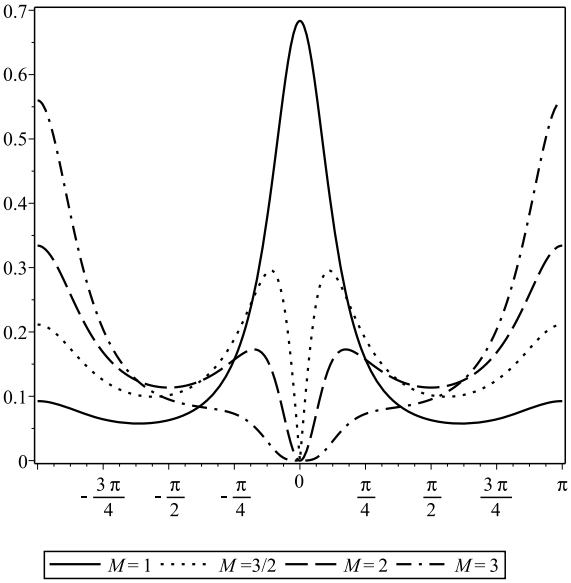

Figure 9: $\zeta = 1/2, r = \lambda = \gamma = 1, \mu = 0$

3.3.2 The Pearson type VII generalization $\mathrm{vMd}_{g_P;\zeta,r,\lambda,\mu,\alpha}$

In addition to the parameters (ζ, r, λ), the Pearson VII type dgf g_P brings along the parameters $M > 1$ and $m > 0$. We put $m = 1$ because replacing (r, λ, m) by $(r/\sqrt{m}, \lambda/\sqrt{m}, 1)$ yields the same density. Again, one can model uni- and bimodality as well as symmetry and asymmetry, see Figures 10 up to 13. A bit more general discussion of the question which influence light and heavy bivariate elliptically contoured distribution tails have onto the shape of the generalized vMd is provided in the next section.

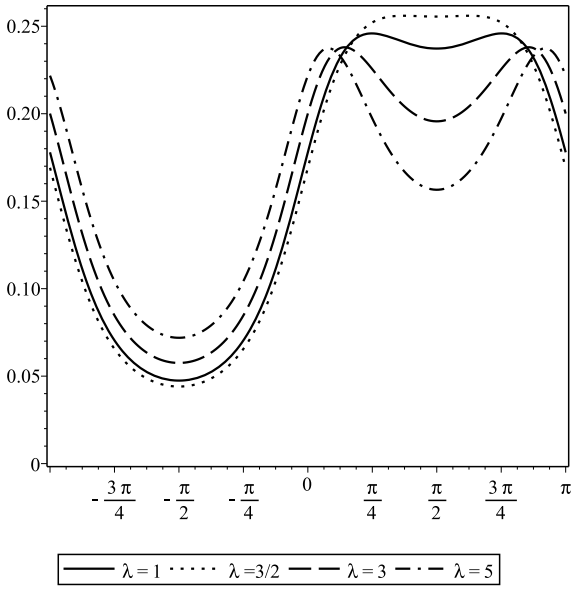

Figure 10: $\zeta = 2/3, r = 1 = M, \mu = \pi/2$

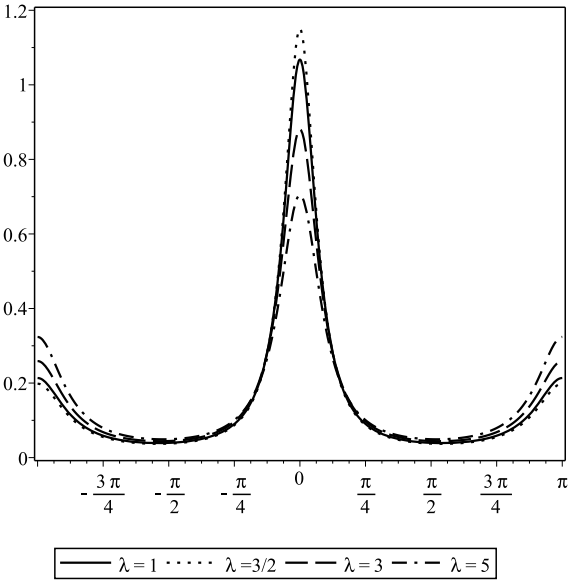

Figure 11: $\zeta = 1/3, r = 1 = M, \mu = 0$

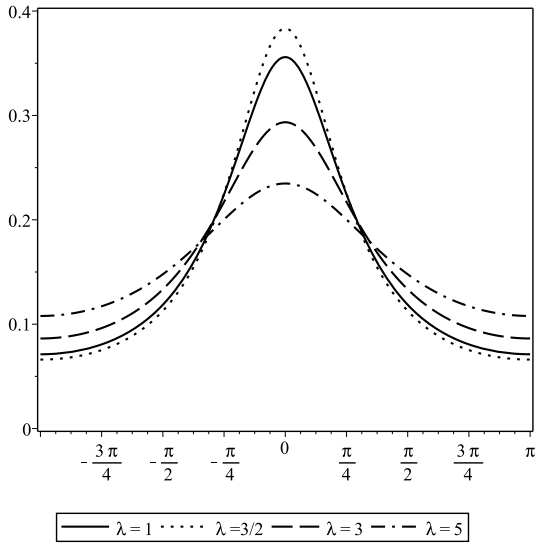

Figure 12: $\zeta = 1 = r = M, \mu = 0$

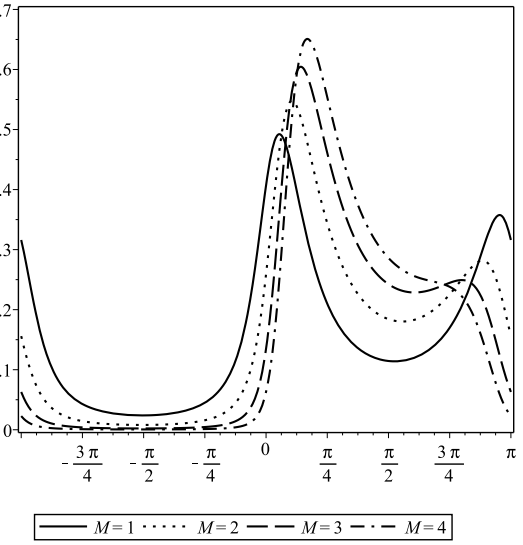

Figure 13: $\zeta = 1/3, r = \lambda = 1, \mu = \pi/3$

3.3.3 Light and heavy bivariate distribution tails and mass concentrations

Notice that $\varphi \mapsto 1/(2\pi\,\zeta\,N^2_{(1,\zeta)}(\varphi - \alpha))$ is the circular pdf corresponding to the $E_{(1,\zeta)}$-generalized uniform probability distribution on the Borel sets of $E_{(1,\zeta)}$ introduced in Richter [2011a], shifted by $\alpha \in [0, \pi)$. This function reduces to the pdf of the circular uniform distribution if ζ attains the value 1, see Figure 14. Hence, the pdf in (12) can be considered as the shifted circular $E_{(1,\zeta)}$-generalized uniform distribution, perturbated by the factor involving g.

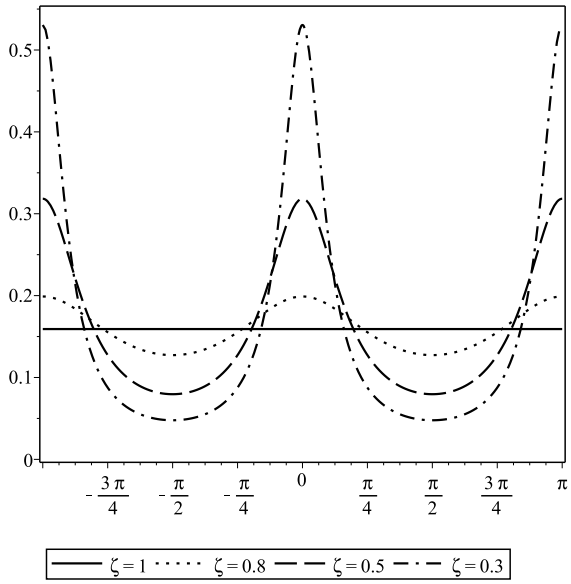

Figure 14: $E_{(1,\zeta)}$-generalized uniform distribution

Recall that the argument of the dgf g in the representation (12) of the regular elliptically contoured g-generalization of the vMd takes values only in the interval $[\lambda - r, \lambda + r]$ where the boundaries are attained if $\varphi = \mu + \pi$ or $\varphi = \mu$, respectively. Consequently, the bivariate distribution's tail effects the shape of the generalized vMd most if $\lambda \gg r$. If r and λ are close to each other and not very far from zero then the shape of the generalized vMd is mostly effected by the distribution's probability mass around its expectation vector ν. Finally, if λ and r are close to each other and $\lambda + r \gg 0$ then the portion of the bivariate distribution's probability mass effecting the generalized vMd is largest and the shape of the generalized vMd may be effected by the two-dimensional

distribution's center as well as by its tail.

If $r = \lambda = 1$ then the argument of g is restricted in (12) to the interval $[0, 2]$. In Figure 15, the restrictions of the dgfs g_K and g_P to this interval are visualized where w.l.o.g. β and m are chosen as $\beta = 1/2$ and $m = 1$, respectively. In the case of the Kotz type dgf, large values of the parameter M 'prefer' directions close to μ which correspond to arguments of g close to the number two. Moreover, large values of the parameter γ split the interval $[-\pi, \pi)$ into two portions, one which 'prefers' the corresponding directions and one which gives lower weight to its corresponding directions. Considering g_P, large values of M of m yield large values of g if φ is close to $\mu + \pi$.

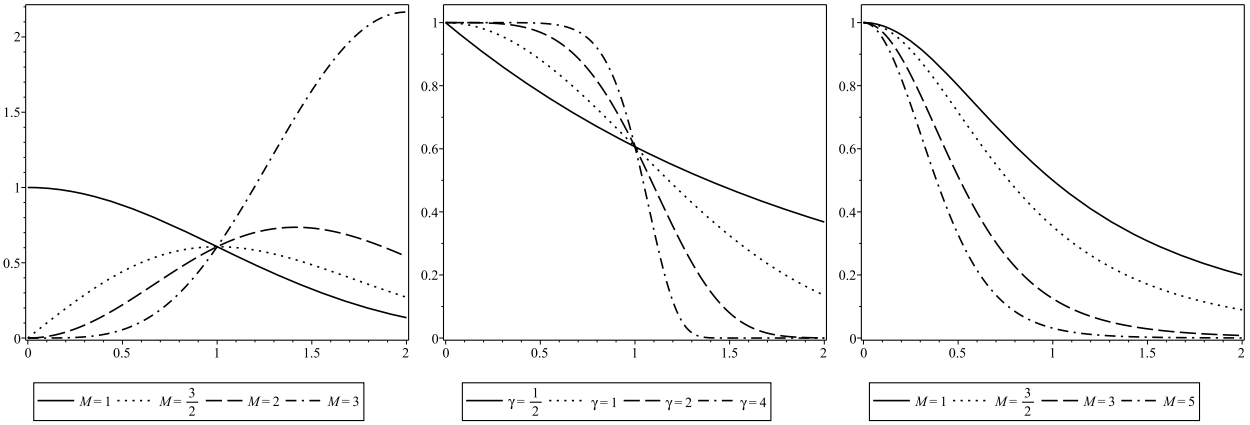

Figure 15: left: g_K, where $\beta = \frac{1}{2}$ and $\gamma = 1$ center: g_K, where $M = 1$ and $\beta = \frac{1}{2}$
right: g_P, where $m = 1$

4 Star-shaped models

Let $K \subset \mathbb{R}^2$ be a star body having the origin 0_2 as an inner point. Hence, K is compact and equal to the closure of its interior, $kerK$ is not empty and $0_2 \in kerK$ where $kerK$ stands for the set of all points w.r.t. which K is star-shaped. Recall that K is said to be star-shaped w.r.t. a point $a \in K$ whenever for every $x \in K \setminus \{a\}$ the segment with the endpoints a and x is contained in K. For such K, the Minkowski functional $h_K : \mathbb{R}^2 \to [0, \infty)$ is well defined. We assume that h_K is positively homogeneous and call $K(r) = rK = \{(x, y)^T \in \mathbb{R}^2 : h_K((x, y)^T) \leq r\}$ and its topological boundary $S(r) = rS$ the star ball and star sphere of star radius or Minkowski radius $r > 0$, respectively. A special case which may be of interest for its own is given if K is a ball w.r.t. any norm in $\mathbb{R}^2$.

In slightly other notation than in Richter [2011b], let $\sin_K(\varphi) = \sin\varphi/M_K(\varphi)$, $\cos_K(\varphi) = \cos\varphi/M_K(\varphi)$ denote star-generalized trigonometric functions, where $M_K(\varphi) = h_K((\cos\varphi, \sin\varphi)^T)$. Note that the star body corresponding to a bivariate elliptically contoured distribution is the disc K_Σ having the ellipse E_Σ as its topological boundary. Also note that the special definition of the $E_{(a,b)}$-generalized trigonometric functions in Section 2 slightly differs from the present general definition of the star-generalized trigonometric functions by the scaling factors $1/a$ and $1/b$.

Generalizing the conditional offset approach described in Section 2, the following star-shaped generalized vMd was derived in Richter [2014]

$$\mathrm{vMd}_{g;K,r,\lambda,\mu}(\varphi) = D(g, K) R_S^2(\varphi) g\left(h_K\left(\begin{pmatrix} r\cos_K(\varphi) - \lambda\cos_K(\mu) \\ r\sin_K(\varphi) - \lambda\sin_K(\mu) \end{pmatrix}\right)\right), \tag{16}$$

where g is a dgf, R_S describes S by $S = \left\{R_S(\varphi)\begin{pmatrix}\cos\varphi \\ \sin\varphi\end{pmatrix}, \varphi \in [-\pi, \pi)\right\}$, and

$$D(g, K) = \left(\int_{-\pi}^{\pi} R_S^2(\varphi) g\left(h_K\left(\begin{pmatrix} r\cos_K(\varphi) - \lambda\cos_K(\mu) \\ r\sin_K(\varphi) - \lambda\sin_K(\mu) \end{pmatrix}\right)\right) d\varphi\right)^{-1}. \tag{17}$$

Note that $h_K((x,y)^T) = 1$ for $(x,y)^T \in S$ implies that $M_K(\varphi) = 1/R_S(\varphi)$. For proving formula (16), it was supposed in Richter [2014], Section 2, that a certain Assumption 1 w.r.t. the boundary S of K is satisfied. Since this is the case in all examples considered in the present paper, we will not introduce the details of this assumption. Instead, we draw some consequences from formula (16) in the subsequent sections. To this end, we have inter alia to derive explicit expressions for the Minkowski functionals of several star bodies. Having done this, (16) gives further generalizations of the vMd. Note that formally defining a probability dgf on a circle might be done without considering the normalizing constant associated with it. It is therefore another key point of the present conditional offset approach to give the explicit representation of the normalizing constant in (17).

5 Visualization of the star-shaped generalized vMd

As mentioned before, determining an explicit expression for the Minkowski functional of the underlying star body K plays the key role in deriving a concrete star-shaped generalized vMd from the general formula (16). This way a non-concentric elliptically contoured, a polygonally contoured and a p-generalized elliptically contoured generalization of the vMd is derived in this section.

5.1 Non-concentric elliptically contoured generalization

In this section, we assume that the star body K is an elliptical disc containing the origin as an arbitrary inner point not necessarily being a center of symmetry,

$$K = K_{a,b;e,f} = \left\{(x,y)^T \in \mathbb{R}^2 : |(x+e, y+f)^T|_{(a,b)} \leq 1\right\}.$$

Proposition 1. The Minkowski functional of the shifted elliptical disc is

$$h_{K_{a,b;e,f}}((x,y)^T) = \frac{\frac{ex}{a^2} + \frac{fy}{b^2} + \sqrt{\frac{x^2}{a^2} + \frac{y^2}{b^2} - \frac{(fx-ey)^2}{a^2b^2}}}{1 - \frac{e^2}{a^2} - \frac{f^2}{b^2}},\ (x,y)^T \in \mathbb{R}^2.$$

Proof. Starting from the definition

$$h_K((x,y)^T) = \inf\left\{\lambda > 0 : (x,y)^T \in \lambda K\right\}, (x,y)^T \in \mathbb{R}^2,$$

it follows that

$$\begin{aligned}
h_{K_{a,b;e,f}}((x,y)^T) &= \inf\left\{\lambda > 0 : \frac{\left(\frac{x}{\lambda} + e\right)^2}{a^2} + \frac{\left(\frac{y}{\lambda} + f\right)^2}{b^2} \leq 1\right\} \\
&= \inf\left\{\lambda > 0 : b^2(x+\lambda e)^2 + a^2(y+\lambda f)^2 \leq a^2b^2\lambda^2\right\} \\
&= \inf\left\{\lambda > 0 : (a^2f^2 + b^2e^2)\lambda^2 + 2(b^2ex + a^2fy)\lambda + b^2x^2 + a^2y^2 \leq a^2b^2\lambda^2\right\} \\
&= \inf\left\{\lambda > 0 : (a^2b^2 - a^2f^2 - b^2e^2)\lambda^2 - 2(b^2ex + a^2fy)\lambda - b^2x^2 - a^2y^2 \geq 0\right\}.
\end{aligned}$$

Because we assumed that $(0,0)^T$ is an inner point of K,

$$1 > |(e,f)^T|_{(a,b)} = \frac{e^2}{a^2} + \frac{f^2}{b^2}.$$

Consequently, the set of points satisfying the equation

$$(a^2b^2 - a^2f^2 - b^2e^2)\lambda^2 - 2(b^2ex + a^2fy)\lambda - b^2x^2 - a^2y^2 = 0$$

is an open up parabola with two real valued roots, say $\lambda_{1,2}$,

$$\begin{aligned}
\lambda_{1,2} &= \frac{(b^2ex + a^2fy) \oplus \sqrt{(b^2ex + a^2fy)^2 + (b^2x^2 + a^2y^2)(a^2b^2 - a^2f^2 - b^2e^2)}}{a^2b^2 - a^2f^2 - b^2e^2} \\
&= \frac{\frac{ex}{a^2} + \frac{fy}{b^2} \oplus \sqrt{\frac{x^2}{a^2} + \frac{y^2}{b^2} - \frac{(fx-ey)^2}{a^2b^2}}}{1 - \frac{e^2}{a^2} - \frac{f^2}{b^2}},
\end{aligned}$$

where $\oplus$ is accordingly to be chosen as $+$ and $-$. The denominator of the last ratio is greater than zero by assumption, hence for giving a positive solution for λ, the numerator has to be positive, too. Therefore, one has to chose $\oplus$ as $+$. □

Before we visualize the non-concentric elliptically contoured generalized vMd, let us consider the underlying bivariate distributions which are of interest on their own. To this end, let the random vector $(X,Y)^T$ have the pdf

$$\varphi_{g;a,b,e,f}(x,y) = C(g,K_{a,b;e,f}) \cdot g\big(h_{K_{a,b;e,f}}((x-\nu_1, y-\nu_2)^T)\big)\,.$$

According to Richter [2014], the random vector $(X,Y)^T$ follows a non-centric elliptically contoured distribution, $(X,Y)^T \in \mathrm{NCEC}$, where

$$\mathrm{NCEC} = \{(X,Y)^T\colon\ (X,Y)^T \text{ has pdf } \varphi_{g;a,b,e,f},\ g \text{ is any dgf},\ 0<b<a,\ 0<|(e,f)^T|_{(a,b)}<1,\ (\nu_1,\nu_2)^T \in \mathbb{R}^2\}.$$

Proposition 2. The normalizing constant $C(g,K_{a,b;e,f})$ does neither depend on e nor on f, and

$$C(g,K_{a,b;e,f}) = C(g,K_{a,b}) = \frac{1}{I(g)\cdot 2\pi\, ab}\,.$$

Proof. Note that $(\nu_1,\nu_2)^T$ is a vector of location and does not effect the value of $C(g,K_{a,b;e,f})$. Hence, w.l.o.g., $(\nu_1,\nu_2)^T = (0,0)^T$. Following Richter [2014], the normalizing constant satisfies

$$C(g,K_{a,b;e,f}) = \frac{1}{I(g)\cdot \int_0^{2\pi}\left(M_{K_{a,b;e,f}}(\varphi)\right)^{-2}\,d\varphi}\,.$$

The value of the integral coincides with the $E_{a,b;e,f}$-generalized circumference of the topological boundary $E_{a,b;e,f}$ of $K_{a,b;e,f}$. Hence,

$$\begin{aligned}\int_0^{2\pi} \frac{1}{M^2_{K_{a,b;e,f}}(\varphi)}\,d\varphi &= \frac{d}{d\rho}\lambda(K_{a,b;e,f}(\rho))\mid_{\rho=1}\\ &= \frac{d}{d\rho}\lambda(\rho\, K_{a,b;e,f})\mid_{\rho=1} = 2\,\lambda(K_{a,b;e,f}) = 2\,\lambda(K_{a,b}) = 2\pi\, ab,\end{aligned}$$

where λ denotes the Lebesgue measure on $\mathbb{R}^2$, and

$$C(g,K_{a,b;e,f}) = \frac{1}{I(g)\cdot 2\pi\, ab}.$$

□

The non-centric nature of such a distribution is shown in Figure 16 where the random vector's density level sets are plotted next to its pdf. The same figure also visualizes the corresponding Gaussian non-concentric elliptically contoured generalization of the vMd.

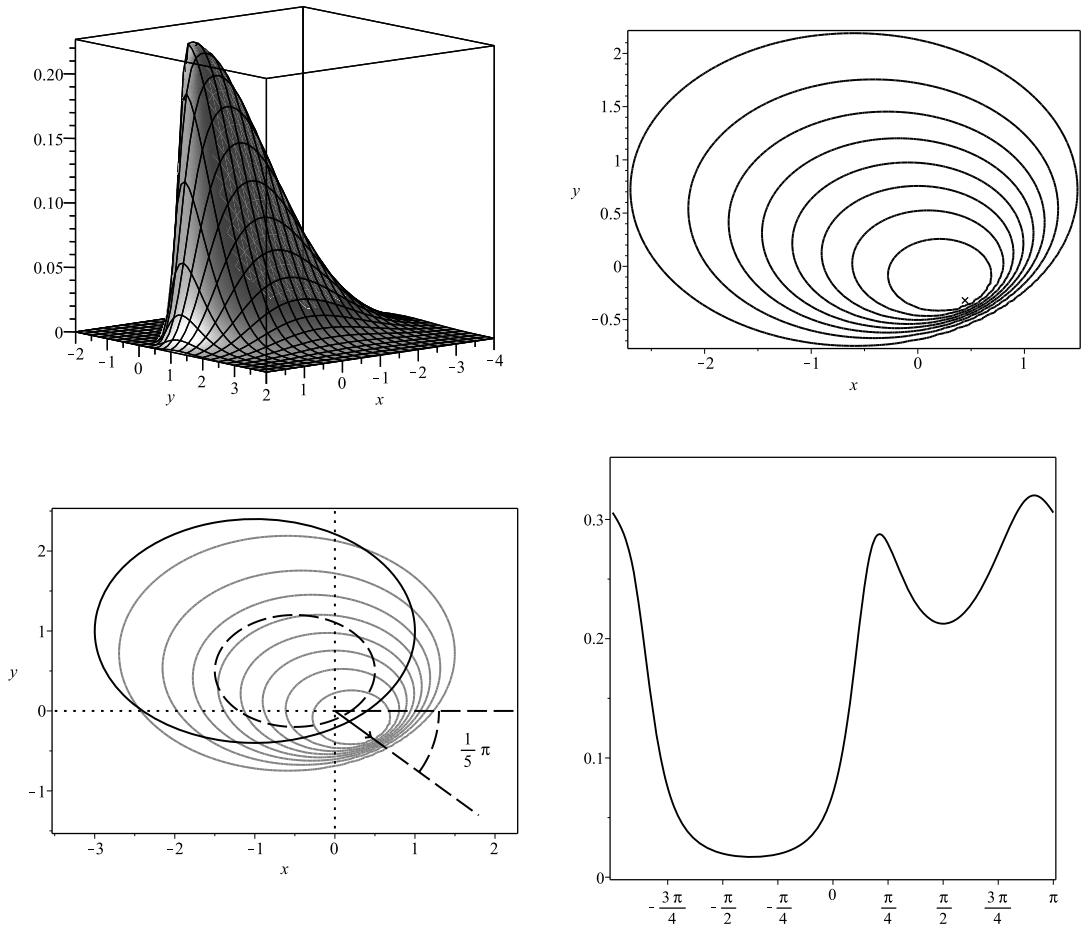

Figure 16: top: The pdf $\varphi_{g;a,b,e,f}(x,y)$ and the corresponding non-concentric density level sets where $g = g_G$, $a = 1$, $b = 0.7$, $e = 0.5$, $f = -0.5$, $\mu = -\pi/5$, $\lambda = 5$ and $(\nu_1, \nu_2) = \lambda(\cos_{K_{a,b;e,f}}(\mu), \sin_{K_{a,b;e,f}}(\mu)) \approx (0.449, -0.326)$.
bottom: The circular pdf derived by the conditional offset approach in the same constellation of parameters, and where $r = 2$.

If we put $\mu = \pi/4$ and leave all other parameters unchanged, the shape of the non-concentric elliptically contoured generalized vMd changes significantly, see Figure 17. Further non-concentric elliptically contoured generalized vMds are visualized in Figures 18 and 19 in the case $g = g_G$, $r = \lambda = 1$ and $\mu = 0$.

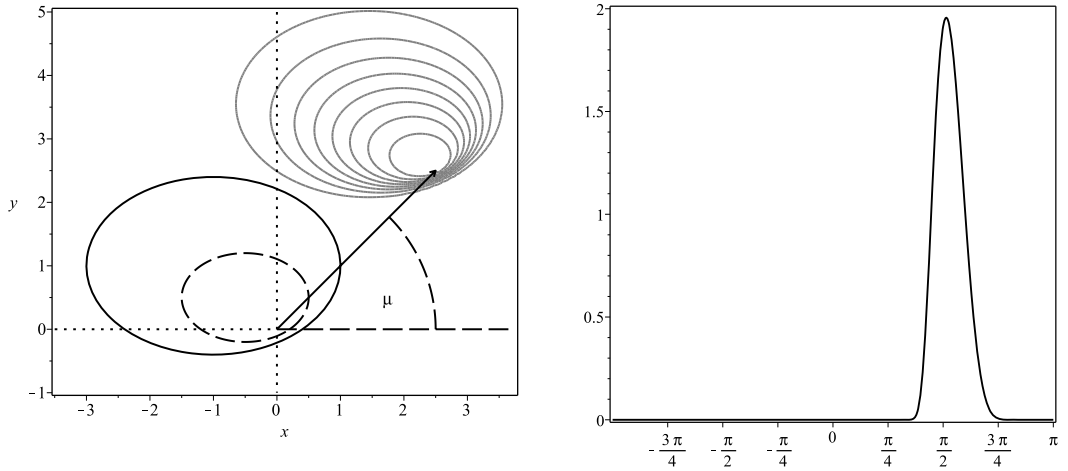

Figure 17: The circular pdf derived by the conditional offset approach, where $r = 2$ and $\mu = \pi/4$.

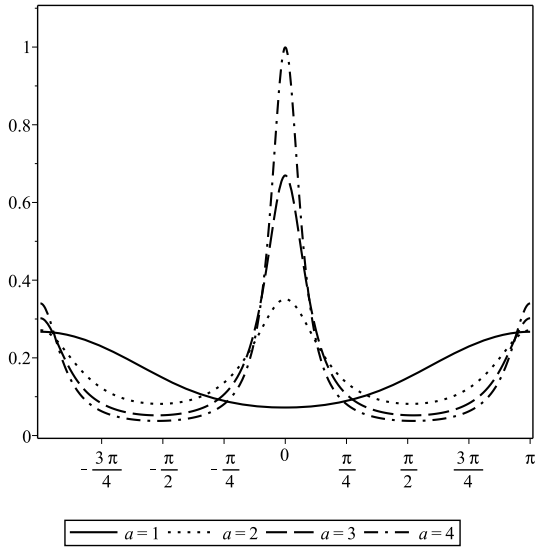

Figure 18: $b = 1$, $e = 0.5$, $f = 0$

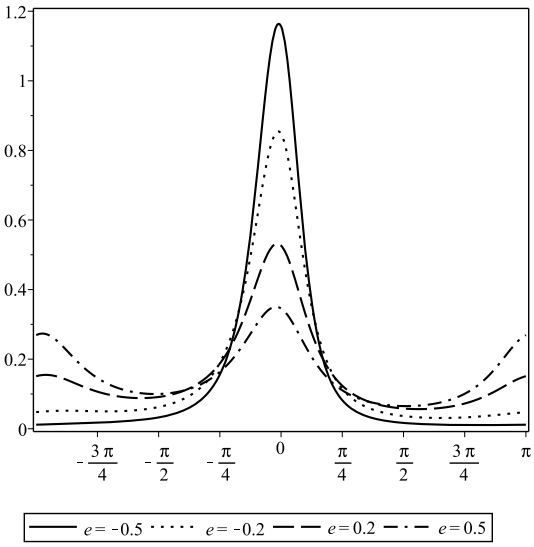

Figure 19: $a = 2$, $b = 1$, $f = 0.1$

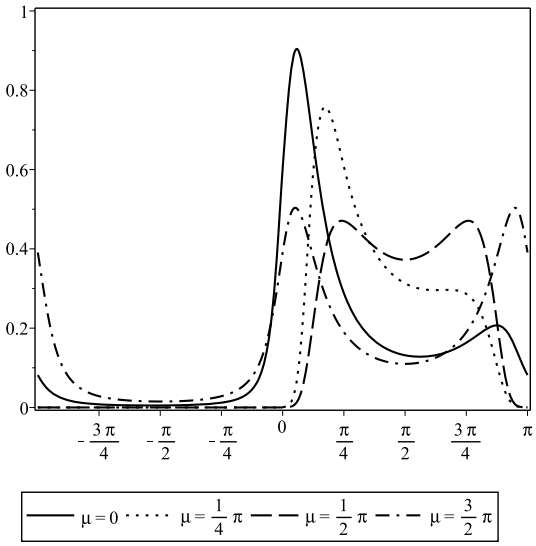

Figure 20: Non-concentric elliptically contoured generalized $\text{vMd}_{g;K_{a,b;e,f},r,\lambda,\mu}$ with $g = g_G$, $a = 1$, $b = \frac{1}{3}$, $e = 0$, $f = -\frac{1}{5}$ and $r = \lambda = 1$.

Remark 2. For given circular data, one might be interested in finding a suitable star body K to construct a suitable model based upon a star-shaped generalized vMd as in (16). One might come up with an idea on such a star body if one plots a rose diagram based upon the data. Then, one of the easiest star-shaped generalized vMd one can think of could be

$$\mathrm{vMd}_K(\varphi) = D(K) \cdot R_S^2(\varphi)\,. \tag{18}$$

Note that (18) is closely related to the star-generalized uniform probability distribution ω_S and the Lebesgue measure of the so called star sectors of the corresponding star body K. For more details on star sectors and ω_S, we refer to Richter [2014]. Figure 21 shows the rose diagrams to the data sets from Section 3, where the number of circular segments corresponds to the number of bins for the histograms there. The diagrams are normed such that the total area of all circular segments in each diagram equals one. From these figures, one might get the impression that a non-concentric and rotated ellipse with half main axes of length 1 and ζ would be a suitable star body for modeling the given data. That is why we do not fit (18) directly to the data, but the density in (18), modified by the additional shift parameter $\alpha \in [0, \pi)$,

$$\mathrm{vMd}_K(\varphi - \alpha) = D(K) \cdot R_S^2(\varphi - \alpha). \tag{19}$$

In other words, we are maximizing the logarithmic likelihood over the parameter set $\{\zeta, e, f, \alpha\}$.

Possible points of further investigation are the following two empirical oberservations. Several graphs of the densities (19) seem to be quite similar to those of model (7). Moreover, the corresponding logarithmic likelihoods are close to those in Table 2. The geometric aspect of the interpretation of our models is additionally supported by plotting the ellipses in Figure 21. Notice that the ellipses are normalized such that their enclosed area equals one.

Table 2: ML estimates of the parameters and the maximized log-likelihood

model (19)	$\hat{\zeta}$	$\hat{e}$	$\hat{f}$	$\hat{\alpha}$	l
Pan Arctic basins	0.2159	0.4674	0.0178	0.9898	−337.1157
Europe basins	0.2705	0.1827	0.0127	0.8500	−492.5067
Greenland basins	0.2929	-0.0070	0.0361	0.9353	−544.1263
North America basins	0.2065	0.1476	0.0152	1.0199	−440.3759
Neuglobsow	0.5536	0.4437	-0.2011	1.8005	−1008.2793

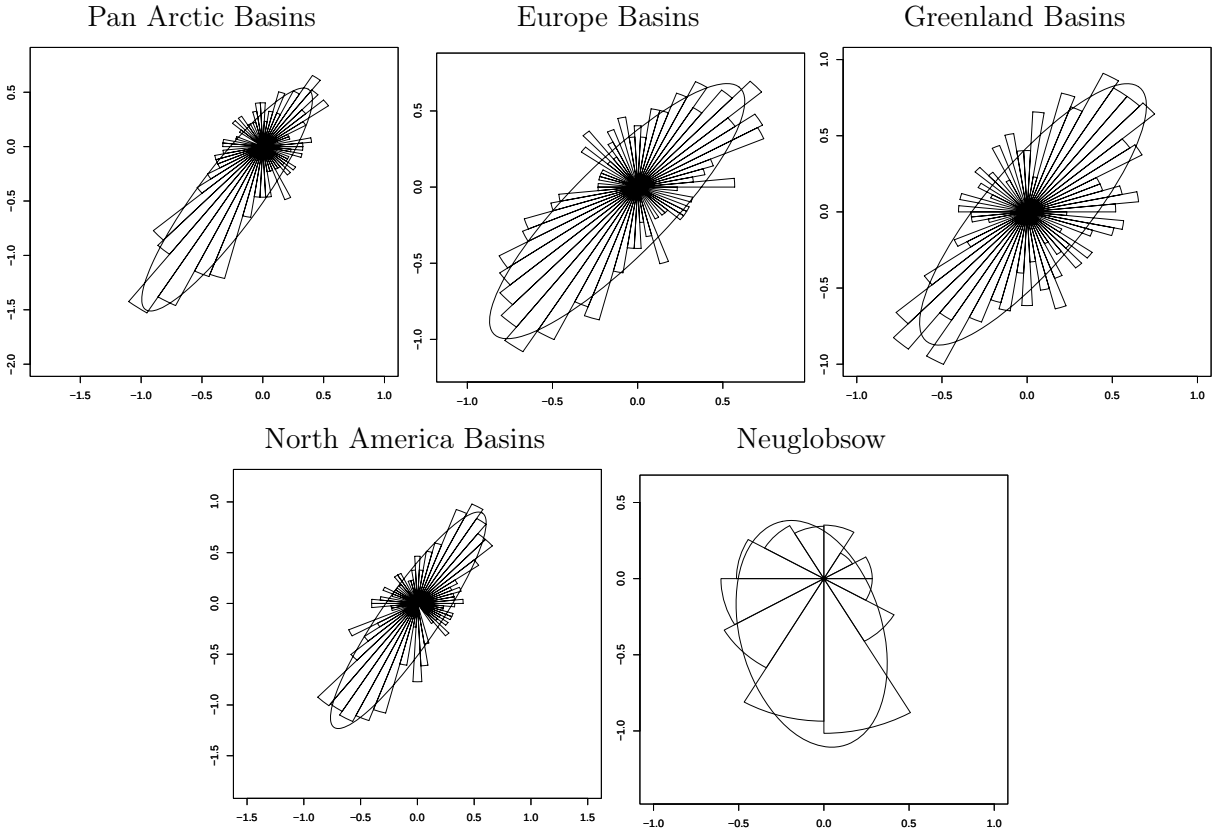

Figure 21: Rose diagrams and the fitted density as in (19)

5.2 Polygonally contoured generalization

Regular convex polygons P_n having n vertices and the convex star body K_n circumsribed by P_n are dealt with in Richter and Schicker [2016]. There, the authors give a polygonal disintegration formula of the Lebesgue measure, and derive normalizing constants of dgfs in dependence of polygonal circle numbers being themselves generalizations of the well known circle number π. To this end, the authors derive the following Minkowski functional of K_n,

$$h_{K_n}((x,y)^T) = \sum_{i=1}^{n} \mathbb{1}_{[2\pi(i-1)/n, 2\pi i/n)}(\mathrm{Pol}^{*-1}(x,y)) \, \frac{x\cos((2i-1)\pi/n) + y\sin((2i-1)\pi/n)}{\cos(\pi/n)} \,,$$

$(x,y)^T \in \mathbb{R}^2$, where $\mathrm{Pol}^{*-1}(x,y)$ again denotes the polar angle, i.e. the angle between the positive x-axis and the ray starting in the origin and passing through the point (x,y). Figure 22 shows the circular pdf $\varphi \mapsto C_n/M_{K_n}^2(\varphi)$ corresponding to the polygonally generalized uniform probability distribution on the Borel sets of P_n, where C_n is a norming constant. It also shows the polygonally contoured g_G-generalized vMd for the same values of n. For details on star generalized uniform distributions, we refer to Richter [2014]. The influence of $r > 0$ and $\lambda > 0$, still in the Gaussian case, $g = g_G$, is illustrated in Figure 23.

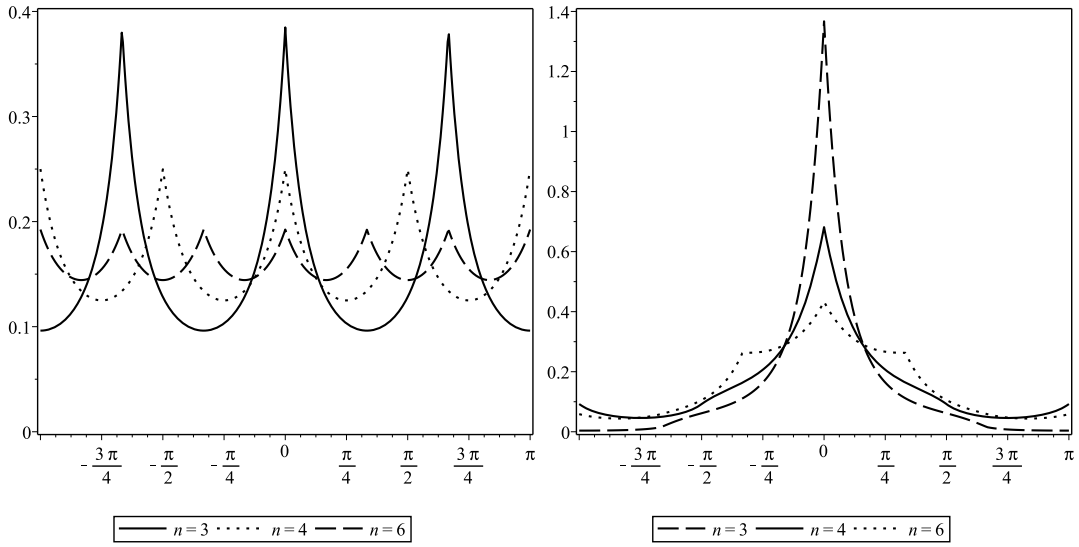

Figure 22: Polygonally generalized uniform distribution [left] and the polygonally contoured generalized $\mathrm{vMd}_{g;K_n,r,\lambda,\mu}$ with $g = g_G$, $r = 1$, $\lambda = 1$ and $\mu = 0$ [right].

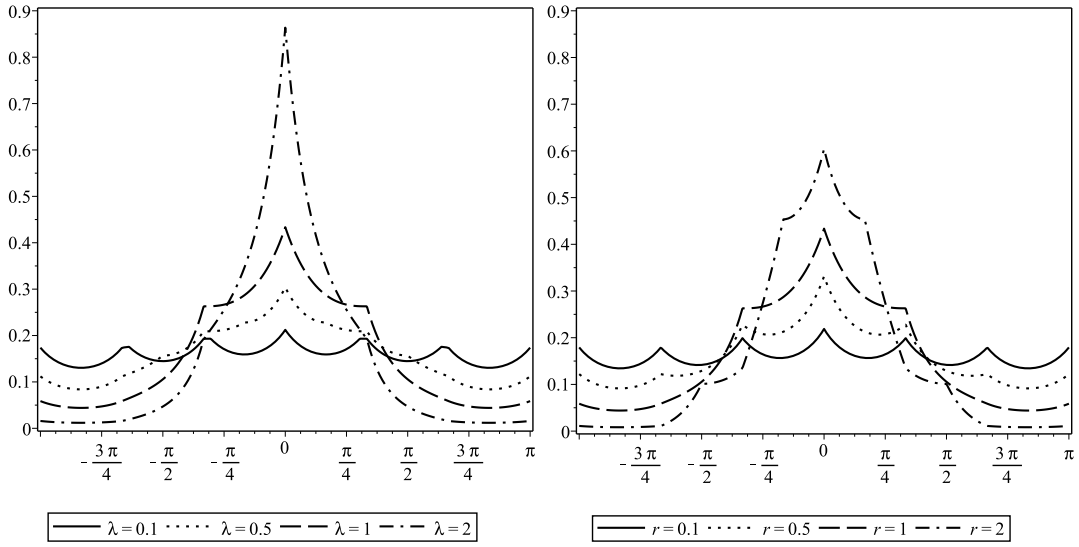

Figure 23: Polygonally contoured generalized $\mathrm{vMd}_{g;K_n,r,\lambda,\mu}$ with $g = g_G$, $n = 6$, $r = \lambda = 1$, and $\mu = 0$ unless stated otherwise.

Example 1 Let a production process P be devided into two consecutive sub-processes P_1 and P_2 each having the same average processing time $T > 0$. The initialization of the sub-process P_2 starts immediately after the termination of P_1. However, the moment of transition from P_1 to P_2 is assumend to be unobservable for some reason. The random deviations T_1^* and T_2^* the processing times of the sub-processes P_1 and P_2 have from T, respectively, are assumed to jointly follow a continuous K_4-shaped distribution with dgf $g : [0, \infty) \to [0, \infty)$ and contour defining star body K_4. In other words, T_1^* and T_2^* have the joint pdf

$$(t_1^*, t_2^*)^T \mapsto C(g, K_4) \cdot g(h_{K_4}((t_1^*, t_2^*)^T)), \quad (t_1^*, t_2^*)^T \in \mathbb{R}^2,$$

where $h_{K_4}((t_1^*, t_2^*)^T) = |t_1^*| + |t_2^*|$, $0 < I(g) < \infty$ and $C(g, K_4)$ is the normalizing constant. It follows from Richter [2009] that the distribution of $(T_1^*, T_2^*)^T$ can also be considered as a continuous $l_{2,1}$-symmetric distribution. Due to initializing processes there is a (non random) delay of ν_1 before P_1 starts and a (non random) delay of ν_2 before P_2 starts, where $\nu_1, \nu_2 \geq 0$. The random vector

$(T_1, T_2)^T := (T_1^* + \nu_1, T_2^* + \nu_2)^T$ has the joint density function

$$(t_1, t_2)^T \mapsto C(g, K_4) \cdot g(h_{K_4}((t_1 - \nu_1, t_2 - \nu_2)^T)) .$$

Hence, we do not recognize the deviation $T_1^* + T_2^*$ from $2T$ but $T_1 + T_2 = T_1^* + \nu_1 + T_2^* + \nu_2$, at the end of the production process.

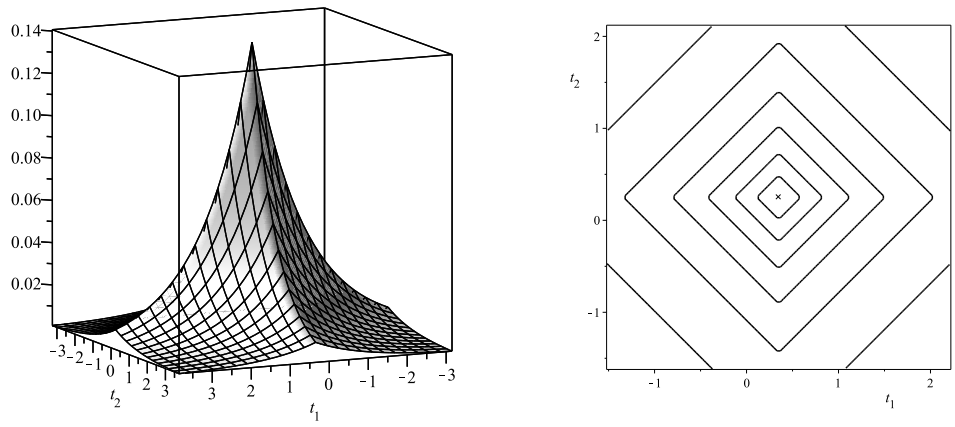

Figure 24: The pdf of $(T_1, T_2)^T$ where $g(r) = e^{-\lambda r}$, $r > 0$, and the corresponding density level sets.

Moreover, let the production process be sensitive to the deviation of the sub-processes from their average processing times. Both, 'heavy' downward and upward deviations T_i^* of a single sub-processing time from T, $i \in \{1, 2\}$, may therefore indicate problems in the production process. Hence, the (unobservable) variable $|T_1^*| + |T_2^*|$ may be of special interest. For sufficiently small ν_1 and ν_2 this random variable could be approximated by $|T_1| + |T_2|$.

Assume that the production process P terminated successfully and that $|T_1| + |T_2| = t$, $t > 0$. We consider now the conditional probabilities for that both T_1 and T_2 are positive, T_2 is larger then T_1, and the absolute value of T_2 is greater than that of T_1, each time given that $|T_1| + |T_2| = t$. Any of these conditional probabilities can be evaluated on the basis of the polygonally contoured generalized vMD:

$$\begin{aligned} P(T_1 > 0, T_2 > 0 \mid |T_1| + |T_2| = t) &= P\left(0 < \Phi < \frac{\pi}{2}\right) , \\ P(T_2 > T_1 \mid |T_1| + |T_2| = t) &= P\left(\frac{\pi}{4} < \Phi < \frac{5\pi}{4}\right) , \\ P(|T_2| > |T_1| \mid |T_1| + |T_2| = t) &= P\left(\frac{\pi}{4} < \Phi < \frac{3\pi}{4}\right) + P\left(\frac{5\pi}{4} < \Phi < \frac{7\pi}{4}\right) . \end{aligned}$$

Here, Φ has the circular pdf $\mathrm{vMd}_{g;K_4,r,\lambda,\mu}$ where $r = t$, and $\lambda > 0$ and $\mu \in [-\pi, \pi)$ satisfy

$$\begin{pmatrix} \nu_1 \\ \nu_2 \end{pmatrix} = \lambda \cdot \begin{pmatrix} \cos_{K_4}(\mu) \\ \sin_{K_4}(\mu) \end{pmatrix} .$$

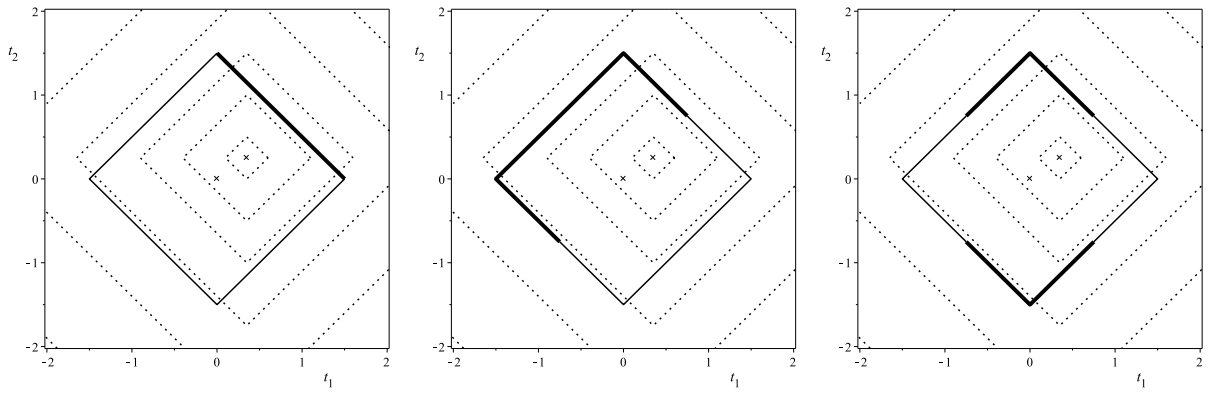

Figure 25: Density level sets of the random vector $(T_1, T_2)^T$ centered at $(\nu_1, \nu_2)^T$ (dotted), the set $t \cdot K_4 = \{(t_1, t_2)^T \in \mathbb{R}^2 : |t_1| + |t_2| = t\}$ (solid, thin) and, from left to right, the subset of all $(t_1, t_2)^T \in t \cdot K_4$ satisfying $t_1 > 0, t_2 > 0$ or $t_2 > t_1$ or $|t_2| > |t_1|$, respectively (solid, thick).

In the same manner, one can evaluate conditional probabilities concerning T_1^* and T_2^* on using $T_i = T_i^* + \nu_i$, $i = 1, 2$. The resulting probabilities are exact even though there might be some more effort in the evaluation of the corresponding set of angles than in the examples in Figure 25.

5.3 The p-generalized elliptically contoured generalization

For some $a, b > 0$, let the disc $K_{a,b;p}$ be circumscribed the p-generalized ellipse

$$E_{a,b;p} = \left\{ (x, y)^T \in \mathbb{R}^2 : \left(\left| \frac{x}{a} \right|^p + \left| \frac{y}{b} \right|^p \right)^{\frac{1}{p}} = 1 \right\}.$$

Then, according to Richter [2014],

$$h_{K_{a,b;p}}((x, y)^T) = \left(\left| \frac{x}{a} \right|^p + \left| \frac{y}{b} \right|^p \right)^{\frac{1}{p}}, \ (x, y)^T \in \mathbb{R}^2 .$$

Figures 26 up to 28 illustrate the resulting generalized $\mathrm{vMd}_{g;K_{a,b;p},r,\lambda,\mu}$ where $g = g_G$. Both sides of Figure 28 illustrate the density for the same choice of parameters except for the parameter $p > 0$. The star body $K_{a,b;p}$ generates a norm, $h_{K_{a,b;p}}$, iff $p \geq 1$. Moreover, if we consider $p \in (0, 1)$, see the right side in Figure 28, then $K_{a,b;p}$ is radially concave with respect to the canonical fan, and generates an antinorm, $h_{K_{a,b;p}}$, see Moszyńska and Richter [2012].

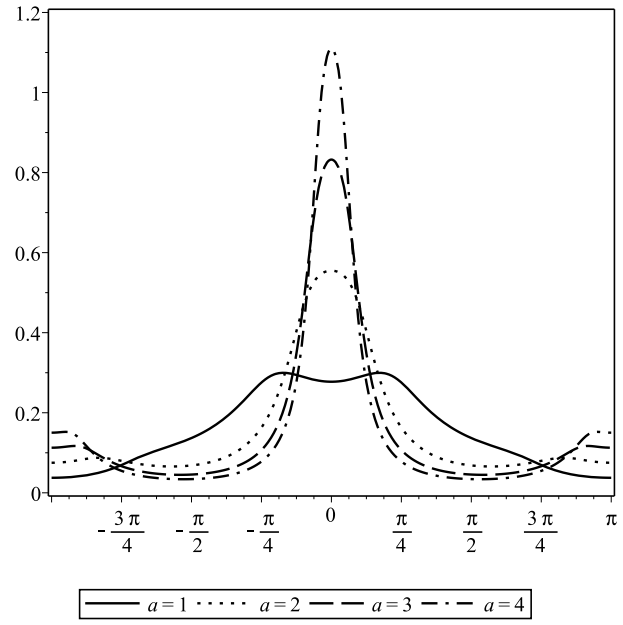

Figure 26: $b = 1, p = 4, r = \lambda = 1, \mu = 0$

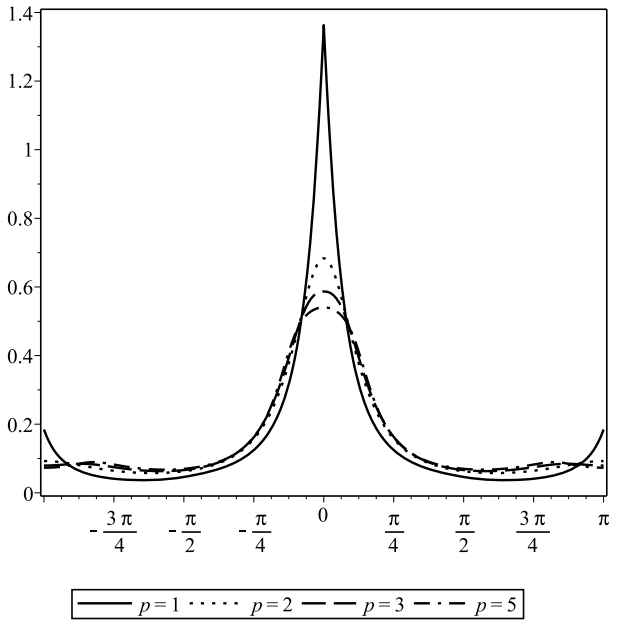

Figure 27: $a = 2, b = r = \lambda = 1, \mu = 0$

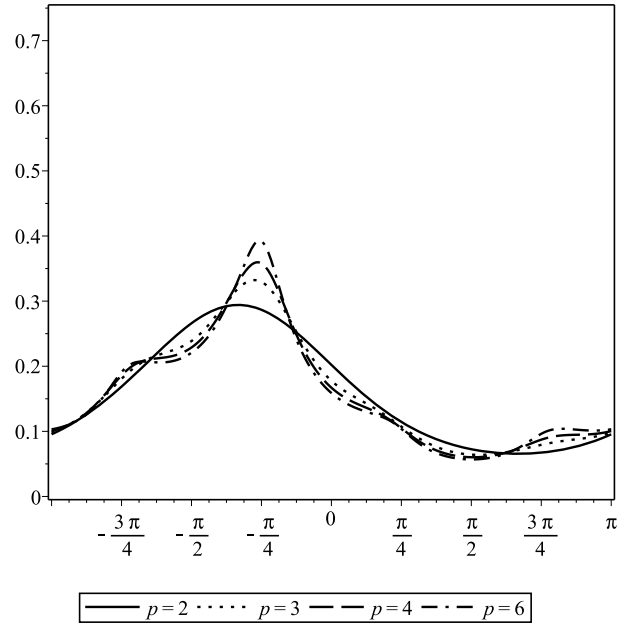

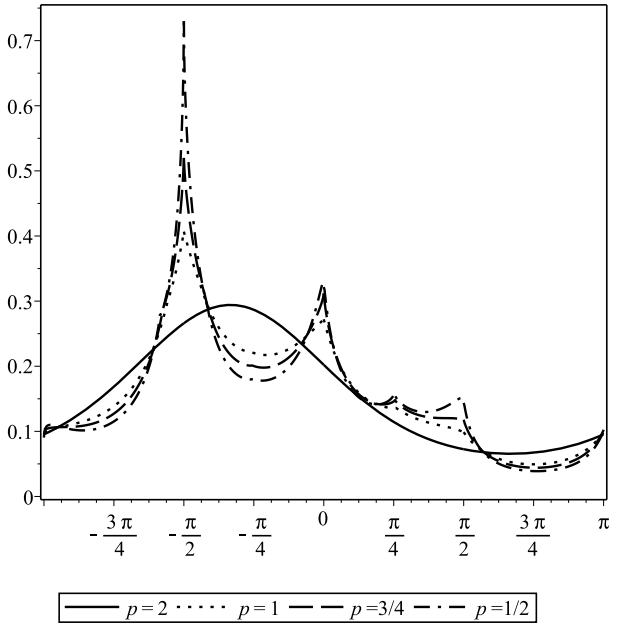

Figure 28: $a = b = 1, r = 3/4, \lambda = 1, \mu = 5\pi/3$

6 Remark on identifiability

At several places throughout Section 2 we introduced restrictions on the parameters of the regular elliptically contoured g-generalized vMD to ensure that different choices of the parameters lead to different distributions. We summarize all these restrictions in Remark 3(c) below. Such identifiability is of special interest in statistical inference. Remark 3(a) concerns constructions using star bodies not considered in the present note.

Remark 3. (a) In the context of the star-shaped generalized vMd introduced in Section 4, one has always to discuss the uniqueness of the parameters separately in dependence on the underlying star body.

(b) Regarding the elliptically contoured generalized vMd, one has always to discuss identifiability dependent on the concrete dgf g. We have done so in context of the dgfs g_G, g_K and g_P.

(c) Still regarding the elliptically contoured generalized vMd but concerning arbitrary dgfs, we have discussed general restrictions on the parameters. Those arose as follows: Starting from any shifted elliptically contoured bivariate distribution with dgf g in Section 2.4, we arrived at the regular elliptically contoured g-generalized vMd as in (12). In doing so, we considered the parameters $\lambda > 0$ and $\mu \in [-\pi, \pi)$, $\delta, a, b > 0$ and $\alpha \in [0, \pi/2)$, and $r > 0$, which arose from the expectation vetor ν, the form matrix Θ, and the condition that $R = r$, respectively. Here, we had to restrict the domain of the triple (δ, r, λ), namely $\delta = 1$ and $\lambda \geq r > 0$. In accordance with the introductory axes-aligned Gaussian case in Section 2.1, we enlarged the domain of the angle α, $\alpha \in [0, \pi)$ to restrict a and b to $a \geq b$. Since a and b affect the generalized vMd only through their ratio, we replaced a, b by $\zeta = b/a$, $\zeta \in (0, 1]$.

Acknowledgement The authors are grateful for the reviewers' constructive criticism, which inspired the part of fitting a model to data and comparison of models in Section 3.2.

The second author is also grateful to Arthur Pewsey for the invitation to the International Workshop ADISTA14 in Brussels, May 2014, and thus getting interested in directional distributions.

References

M. Abramowitz and I. A. Stegun, editors. *Handbook of mathematical functions with formulas, graphs, and mathematical tables. 10th printing, with corrections.* National Bureau of Standards. A Wiley-Interscience Publication. New York etc.: John Wiley & Sons. xiv, 1046 pp., 1972.

E. Batschelet. Circular statistics in biology. Mathematics in Biology. London etc.: Academic Press, a Subsidiary of Harcourt Brace Jovanovich, Publishers. XVI, 371 p., 1981.

K. P. Burnham and D. R. Anderson. *Model Selection and Multimodel Inference. A Practical Information-Theoretic Approach.* Springer-Verlag New York, 2nd edition, 2002.

T. Dietrich, S. Kalke, and W.-D. Richter. Stochastic representations and a geometric parametrization of the two-dimensional Gaussian law. *Chilean Journal of Statistics*, 4(2):27–59, 2013.

N. Fisher, T. Lewis, and B. Embleton. Statistical analysis of spherical data. Cambridge etc.: Cambridge University Press. XIV, 329 p. (1987), 1987.

R. A. Fisher. *Statistical Methods and Scientific Inference.* Oliver and Boyd. Edinburgh, 2nd edition, 1959.

R. Gatto and S. R. Jammalamadaka. The generalized von Mises distribution. *Statistical Methodology*, 4:341–353, 2007.

I. Gradshteyn and I. Ryzhik. *Table of integrals, series, and products. Translated from the Russian. Translation edited and with a preface by Alan Jeffrey and Daniel Zwillinger.* Amsterdam: Elsevier/Academic Press, 7th ed. edition, 2007.

E. J. Gumbel, J. A. Greenwood, and D. Durand. The Circular Normal Distribution: Theory and Tables. *Journal of the American Statistical Association*, 48(261):131–152, 1953.

S. R. Jammalamadaka and A. SenGupta. *Topics In Circular Statistics.* World Scientific, 2001.

M. C. Jones and A. Pewsey. A family of symmetric distributions on the circle. *Journal of the American Statistical Association*, 100(472):1422–1428, 2005.

S. Kato and M. C. Jones. A Family of Distributions on the Circle With Links to, and Applications Arising From, Möbius Transformation. *Journal of the American Statistical Association*, 105(489): 249–262, 2010.

P. Langevin. Magnétisme et théorie des électrons. *Ann. de Chim. et Phys. (8)*, 5:70–127, 1905.

K. V. Mardia. *Statistics of Directional Data*. Academic Press, 1972.

K. V. Mardia and P. E. Jupp. *Directional Statistics*. John Wiley & Sons, 2000.

M. Moszyńska and W.-D. Richter. Reverse triangle inequality. Antinorms and semi-antinorms. *Stud. Sci. Math. Hung.*, 49(1):120–138, 2012.

A. Pewsey, M. Neuhäuser, and G. D. Ruxton. *Circular statistics in R*. Oxford: Oxford University Press, 2013.

W.-D. Richter. Continuous $l_{n,p}$-symmetric distributions. *Lithuanian Mathematical Journal*, 49: 93–108, 2009.

W.-D. Richter. Ellipses numbers and geometric measure representations. *J. Appl. Anal.*, 17(2): 165–179, 2011a.

W.-D. Richter. Circle numbers for star discs. *ISRN Geometry.*, 2011:16, 2011b.

W.-D. Richter. Geometric disintegration and star-shaped distributions. *Journal of Statistical Distributions and Applications*, 1:20, 2014.

W.-D. Richter. Norm contoured distributions in R^2. *Lecture Notes of Seminario Interdisciplinare di Matematica*, 12:179–199, 2015.

W.-D. Richter and K. Schicker. Circle numbers of regular convex polygons. *Results. Math. Online First*, 2016.

K. Shimizu and K. Iida. Pearson type VII distributions on spheres. *Communications in Statistics - Theory and Methods*, 31(4):513–526, 2002.

R. von Mises. Über die „Ganzzahligkeit“ der Atomgewichte und verwandte Fragen. *Physikalische Zeitschriften*, XIX:490–500, 1918.